

Phonon impact on the coherent control of quantum states in semiconductor quantum dots

Anna Grodecka¹, Lucjan Jacak¹,
Paweł Machnikowski^{1,2}, and Katarzyna Roszak¹

¹Institute of Physics, Wrocław University of Technology,
50-370 Wrocław, Poland

²Institut für Festkörpertheorie, Westfälische Wilhelms-Universität,
48149 Münster, Germany

Abstract

This chapter is devoted to the recent theoretical results on the optical quantum control over charges confined in quantum dots under influence of phonons. We show that lattice relaxation processes lead to decoherence of the confined carrier states. The theoretical approach leading to a uniform, compact description of the phonon impact on carrier dynamics, perturbative in phonon couplings but applicable to arbitrary unperturbed evolution, is described in detail. Next, some applications are presented: phonon damping of Rabi oscillations in quantum dots and phonon-induced error of a single-qubit gate for an excitonic quantum dot qubit as well as for a semiconductor quantum dot spin qubit operated via a STIRAP transfer.

1 Introduction

With the state-of-the-art experimental techniques it is possible to control the quantum state of charge carriers in a quantum dot (QD). Many effects known from quantum optics of natural atoms have been demonstrated in these man-made systems: controlled coherent dynamics in these structures has been induced [1], Rabi oscillations have been observed [2–6] and entanglement between states of interacting dots [7] has been demonstrated.

However, unlike their natural counterparts, the artificial atoms are solid-state structures, embedded in the surrounding macroscopic crystal. Therefore, even in top-quality samples, some perturbing interaction effects are inevitable. The mutual influence of lattice deformation (phonons) and charge distributions is one of these inherent effects. There are three major mechanisms of carrier-phonon interaction [8]: (1) Coulomb interaction with the lattice polarization induced by the relative shift of the positive and negative sub-lattices of the polar compound, described upon quantization by longitudinal optical (LO) phonons; (2) deformation potential coupling describing the band shifts due to lattice deformation, i.e. mainly longitudinal acoustical (LA) phonons; (3) Coulomb interaction with piezoelectric field generated by crystal deformation (LA and transversal acoustical, TA, phonons). The latter most effect is weak for globally charge-neutral excitations (e.g. excitons) in some systems, like InAs/GaAs, but may be of more importance for uncompensated charge distributions (e.g. excess electrons) or for the properties e.g. of GaN dots [9,10], where charges are separated by large built-in fields.

The coupling to the lattice degrees of freedom manifests itself in many ways in the spectroscopic properties of QDs. Resonant interaction with LO phonons leads to the extremely pronounced spectrum reconstruction (formation of resonant polarons) [11–14], acoustic and optical phonons provide

Corresponding author; e-mail address: Pawel.Machnikowski@pwr.wrocl.pl

a relaxation channel for carriers [15{17] with an important role played by phonon anharmonicity [18{21], phonon replicas and phonon-assisted transitions are magnified due to resonant interaction with quantized carrier states [22{27].

The perturbing effect of lattice modes has also been observed experimentally as a fast (~ 1 ps) partial decay of coherent optical polarization induced by an ultra-fast laser pulse [28,5]. The theoretical analysis both in the linear regime [29,30] and in the nonlinear case [31,32] shows that this decay should be viewed as a trace of coherent lattice dynamics (due to lattice inertia) rather than as an effect of typical noise. The agreement between the theoretical modeling of carrier-phonon kinetics [32] and the experimental results [28] shows that phonon-related effects play the dominant role in the kinetics of a confined system on picosecond timescales. Phonon effects are also likely to play the leading role in the damping of Rabi oscillations induced optically in a QD [33{35] (although in the current experiments other effects are also important). Due to strong reservoir memory on timescales relevant for these processes, they cannot be fully understood within the Markovian approximations. In particular, the idea of a "decoherence time", with which the control dynamics competes, is misleading [36].

Apart from the general scientific interest, a strong motivation for studying the phonon processes taking place in semiconductor nanostructures comes from the recent proposals for defining a quantum bit (qubit, the basic unit of quantum information) in terms of orbital (charge) degrees of freedom of an exciton confined in a quantum dot [37] or in terms of spin states controlled via conversion to orbital degrees of freedom [38{43]. The recent experimental demonstration of a quantum logic gate operation with charge degrees of freedom in a QD [44] has strengthened this motivation even more. Understanding phonon-induced decoherence processes is essential for practical implementation of these novel ideas and currently seems to be one of the most topical issues in the field.

In order to study the phonon effects for the general coherent-control and quantum information processing schemes, a theoretical method going beyond the perturbative treatment of the external driving is needed. In this chapter, we present one of such methods, treating the Coulomb interactions between the confined carriers and the coupling to the driving field exactly (non-perturbatively), while the phonon coupling is included as a perturbation. Although the range of validity of such a strictly perturbative treatment may be narrower than that of more sophisticated methods (e.g. the cumulant expansion technique [33]), the advantage of the proposed approach is that it yields closed formulas leading to a clear physical interpretation of the phonon decoherence effects.

The chapter is organized as follows: The next section describes the system under study, introduces its model and discusses the unperturbed evolution under special conditions. In the section 3 we describe the various carrier-phonon coupling mechanisms for single carriers and for excitons. The general idea of decoherence due to lattice relaxation is introduced in the section 4. Next, in the section 5 we develop the theoretical treatment for analyzing the phonon-related decoherence for an arbitrary system evolution. This is then applied to the description of phonon damping of Rabi oscillations (section 6), optimization of control for an excitonic QD qubit (section 7) and fidelity of a spin qubit operated via STIRAP transition (section 8). The final section concludes the chapter.

2 The system and the model

The Hamiltonian of the system. We will consider a system of charges confined in a QD, coupled to coherent electromagnetic field and interacting with phonons of the surrounding crystal medium. The Hamiltonian for the system is

$$H = H_C + H_{ph} + H_{int} \quad (1)$$

The first term H_C describes the carrier subsystem together with the external driving field. Throughout this chapter, we will assume that this driving field is strong enough and its quantum fluctuations

may be neglected, so that the field may be modeled classically. Usually, for a confined system only the lowest part of the discrete spectrum is relevant for reasonable pulse durations and intensities, so it is often convenient to assume that the total wavefunctions of the interacting carrier system are known (e.g. from numerical diagonalization [30]) and to express the Hamiltonian in the basis of these eigenstates. Thus, unless explicitly stated otherwise, we will denote the crystal vacuum by $|j_i\rangle$ and the confined exciton states by $|j_i, n\rangle$, $n = 1$.

Numerical calculations for the harmonic confinement model [30] show that the lowest exciton states may be well approximated by products of the electron ground-state harmonic oscillator wavefunction and a hole wavefunction corresponding to one of the low harmonic oscillator levels. This is due to the large hole effective mass compared to that of the electron. For the same reason, even if the geometrical confinement is the same for both particles, the Coulomb interaction shrinks the hole wavefunction while the electron wavefunction is only slightly modified (the electron excitation energy is much larger than Coulomb energy in a typical self-assembled structure). The separation between the ground state and the lowest dark excited state (hole excitation) is usually of several meV, while the closest bright state (the lowest one with the electron in an excited state) lies approximately at 70 meV.

Also, for the structure of excitonic levels as discussed above, the single-exciton assumption is reasonable under excitation with polarized light. Even though excited single-exciton states may be close to the ground state, they are formed by exciting the hole (which is much heavier than the electron), while the electron remains roughly in its ground single-particle state. Creation of a bi-exciton requires much higher energy, sufficient to promote both carriers to excited states.

The second term in (1) is

$$H_{ph} = \sum_k \epsilon_k b_k^\dagger b_k \quad (2)$$

and describes the energies of phonons, b_k^\dagger, b_k being the phonon creation and annihilation operators (branch index will always be included into k , unless explicitly written). Since only long-wavelength phonons are effectively coupled to carriers confined in a QD (see discussion in the next section) we will here always assume linear and isotropic dispersion for acoustic phonons, so that $\epsilon_s(k) = c_s k$, where c_s is the speed of sound for the branch s ($s = l$ for LA, $s = t$ for TA). Also, because the dispersion of the LO phonons is weak around the zone center, the LO phonons ($s = o$) will be assumed dispersionless, $\epsilon_o = \hbar\omega_o$. We will neglect any anharmonicity effects and assume the free harmonic evolution of the lattice subsystem in absence of the carrier-phonon coupling. Only the bulk phonon modes will be included. Although a quantum dot implies certain electrostatic and mechanical discontinuity of the system and the role of confined phonons may be discussed [18,45], invoking bulk phonons is usually sufficient for explanation of experimental features, like e.g. polaron resonances [11,12].

The last term,

$$H_{int} = \sum_{k, m, n=1}^X j_n \ln^0 F_{nn^0}(k) b_k^\dagger + b_k \quad ; \quad F_{nn^0}(k) = F_{nn^0}(-k); \quad (3)$$

is the exciton-phonon interaction expressed in terms of the discrete confined carrier states $|j_i, n\rangle$. Although inter-band phonon terms may appear e.g. as a consequence of strain-dependent inter-band couplings, in the following sections we deal only with intraband phonon effects, so that the interaction Hamiltonian conserves the number of quasiparticles of each kind.

The phonon wavevectors are restricted to the first Brillouin zone. However, modulations of the band structure with spatial periods much smaller than the size of the carrier wavefunction cannot influence the carrier energy. In the harmonic oscillator approximation for carrier confinement, this leads to exponential cut-off of carrier-phonon interaction (explicit formulas are given in the section 3 below) at the frequency $\omega_0' = c/l$, where c is the sound speed, l is the carrier confinement size. Thus, the exciton is effectively coupled only to the long-wavelength part of the phonon modes. On

the other hand, vanishing of the coupling in the limit of $k = 0$ reflects the insensitivity of the system properties to shifting the lattice as a whole. For gapless bosons with linear dispersion, the characteristic frequency determines the reservoir memory times and sets up the timescale of non-Markovian effects, related to "dressing" of the localized carriers with coherent lattice deformation field (see section 4).

Unperturbed resonantly driven evolution Assuming that the laser field couples resonantly only to one transition (say, from the "empty dot" state $|j\rangle$ to the ground exciton state $|l\rangle$) the Hamiltonian for the carrier subsystem may be written

$$H_{C0} = \sum_n E_n |j\rangle\langle n| + \frac{1}{2} f(t) (e^{i\omega t} |l\rangle\langle 0| + e^{-i\omega t} |0\rangle\langle l|) \quad (4)$$

(the energies E_n are defined with respect to the "empty dot" state).

Using the canonical transformation to the "rotating frame", defined by the unitary operator

$$U_{rw} = \exp \left[-i \sum_{n=1}^{\infty} |j\rangle\langle n| \right]; \quad U_{rw} |j\rangle = e^{-i\omega t} |j\rangle; \quad n \geq 1;$$

we obtain from (4)

$$H_C = U_{rw}^\dagger H_{C0} U_{rw} = \sum_{n=1}^{\infty} |j\rangle\langle n| + \sum_{n=1}^{\infty} E_n |j\rangle\langle n| + \frac{1}{2} f(t) (|l\rangle\langle 0| + |0\rangle\langle l|) \quad (5)$$

where $E_n = \omega - E_n$. In the special case of strictly resonant coupling to the ground-state excitonic transition, $\omega = E_1$, so that the detuning from the ground-state transition vanishes, $E_1 = 0$, and $E_n = E_n$ where E_n are the intra-band excitation energies for a single exciton.

Let us denote the evolution operator for the exciton-light system (generated by H_C , without phonon interactions) by $U_0(t;s)$, where $s; t$ are the initial and final times, respectively. In the special case of resonant coupling only between $|j\rangle$ and $|l\rangle$ state the evolution operator may be found explicitly (note that in this resonant case H_C commutes with itself at different times). The result is

$$U_C(t;s) = \cos \frac{\theta(t)}{2} (|0\rangle\langle 0| + |l\rangle\langle l|) - i \sin \frac{\theta(t)}{2} (|0\rangle\langle l| + |l\rangle\langle 0|) + \sum_{n>1}^{\infty} |j\rangle\langle n| e^{-i E_n (t-s)}; \quad (6)$$

where

$$\theta(t) = \int_s^t d\tau f(\tau)$$

is the rotation angle on the Bloch sphere up to time t .

3 Interactions of confined carriers with phonons

For completeness, in this section we summarize the derivation of the coupling constants between the bulk phonon modes and the confined carriers in a polar and piezoelectric semiconductor [8,46,47].

The deformation potential. Any crystal deformation leads to shifts of the conduction (c) and valence (v) bands which are, to the leading order, proportional to the relative volume change. The corresponding contribution to the energy of electrons (e) and holes (h) in the long-wavelength limit is, therefore,

$$H_{e,h}^{(DP)} = E_{c,v} = \epsilon_{e,h} \frac{V}{V};$$

where ϵ_{eh} are the deformation potential constants for electrons and holes and V is the unit cell volume. Using the strain tensor $\hat{\epsilon}$,

$$\epsilon_{ij} = \frac{1}{2} \left(\frac{\partial u_i}{\partial r_j} + \frac{\partial u_j}{\partial r_i} \right);$$

one may write

$$H_{eh}^{(DP)} = \epsilon_{eh} \text{Tr} \hat{\epsilon} = \epsilon_{eh} \mathbf{r} \cdot \mathbf{u}(\mathbf{r});$$

where $\mathbf{u}(\mathbf{r})$ is the local displacement field. The displacement is quantized in terms of phonons,

$$\mathbf{u}(\mathbf{r}) = \frac{1}{N} \sum_{\mathbf{k}} \frac{\hbar}{2V\omega(\mathbf{k})} \hat{\epsilon}_{\mathbf{k}} \cdot \mathbf{b}_{\mathbf{k}} + \mathbf{b}_{\mathbf{k}}^{\dagger} e^{i\mathbf{k} \cdot \mathbf{r}}; \quad (7)$$

where $\omega(\mathbf{k})$ is the frequency for the wavevector \mathbf{k} , $\hat{\epsilon}_{\mathbf{k};s} = \hat{\epsilon}_{\mathbf{k};s}$ is the corresponding real unit polarization vector, and ρ is the crystal density. Only the longitudinal branch contributes to $\mathbf{r} \cdot \mathbf{u}$ in (7) and the interaction Hamiltonian in the coordinate representation for carriers is

$$H_{eh}^{(DP)} = \epsilon_{eh} \frac{1}{N} \sum_{\mathbf{k}} \frac{\hbar \mathbf{k}}{2V\omega(\mathbf{k})} \cdot \mathbf{b}_{\mathbf{k};l} + \mathbf{b}_{\mathbf{k};l}^{\dagger} e^{i\mathbf{k} \cdot \mathbf{r}}. \quad (8)$$

In the second quantization representation with respect to the carrier states this reads

$$\begin{aligned} H_{eh}^{(DP)} &= \sum_{nn^0} \int d^3r \psi_n^{\dagger}(\mathbf{r}) \psi_{n^0}(\mathbf{r}) \mathbf{a}_n^{\dagger} \mathbf{a}_{n^0} = \sum_{nn^0} \int d^3r \psi_n^{\dagger}(\mathbf{r}) V(\mathbf{r}) \psi_{n^0}(\mathbf{r}) \mathbf{a}_n^{\dagger} \mathbf{a}_{n^0} \\ &= \frac{1}{N} \sum_{k,nn^0} \mathbf{a}_n^{\dagger} \mathbf{a}_{n^0} f_{eh,nn^0}^{(DP)}(\mathbf{k}) \cdot \mathbf{b}_{\mathbf{k};l} + \mathbf{b}_{\mathbf{k};l}^{\dagger}; \end{aligned} \quad (9)$$

where

$$f_{eh,nn^0}^{(DP)}(\mathbf{k}) = \epsilon_{eh} \frac{\hbar \mathbf{k}}{2V\omega(\mathbf{k})} F_{nn^0}(\mathbf{k});$$

with the form factor

$$F_{nn^0}(\mathbf{k}) = \int d^3r \psi_n^{\dagger}(\mathbf{r}) e^{i\mathbf{k} \cdot \mathbf{r}} \psi_{n^0}(\mathbf{r}) = F_{nn^0}(\mathbf{k}); \quad (10)$$

The interaction Hamiltonian (9) conforms with the general form assumed in (3).

General properties of the form factors. While the common coefficient of the coupling Hamiltonian contains the fundamental and material-dependent constants and reflects the general electrical and mechanical properties of the semiconductor system, the form factor (10) contains the information about the geometry of the confinement and the resulting properties of wavefunctions. In this sense, it is the "engineerable" part of the carrier-phonon coupling.

From orthogonality of single-particle states one has immediately $F_{nn^0}(0) = \delta_{nn^0}$. If the wavefunctions are localized at a length l , then the extent of the form factor is l . Thus, for carrier states localized in a QD over many lattice sites and smooth within this range, the functions $F_{nn^0}(\mathbf{k})$ will be localized in the \mathbf{k} space very close to the center of the Brillouin zone.

As an example, let us consider the ground state of the harmonic oscillator potential,

$$\psi_0(\mathbf{r}) = \frac{1}{\sqrt{l_x l_y l_z}} \exp \left[-\frac{1}{2} \left(\frac{r_x^2}{l_x^2} + \frac{r_y^2}{l_y^2} + \frac{r_z^2}{l_z^2} \right) \right]; \quad (11)$$

where r_x is the position component in the xy plane and l_x, l_y are the localization widths in-plane and in the growth (z) direction. The corresponding form factor is then easily found to be

$$F_0(\mathbf{k}) = \exp \left[-\frac{k_x^2 l_x^2}{2} - \frac{k_y^2 l_y^2}{2} - \frac{k_z^2 l_z^2}{2} \right]; \quad (12)$$

Piezoelectric interaction. A propagating phonon wave in a piezoelectric medium induces a polarization field which affects the carriers by means of the Coulomb interaction. If the crystal deformation is described by the strain tensor $\hat{\epsilon}$ then the piezoelectric polarization is $P = \hat{d} \hat{\epsilon}$, where \hat{d} is the piezoelectric tensor.

From the Maxwell equation for plane-wave fields (in absence of external charges and currents),

$$\begin{aligned} i\mathbf{k} \cdot \mathbf{E} &= \frac{1}{\epsilon_0} i\mathbf{k} \cdot \mathbf{P}; & i\mathbf{k} \cdot \mathbf{E} &= i\mathbf{k} \cdot \mathbf{B}; \\ i\mathbf{k} \cdot \mathbf{B} &= 0; & \frac{1}{c^2} \frac{d\mathbf{B}}{dt} &= -i\mathbf{k} \times \mathbf{E} - \frac{1}{\epsilon_0} i\mathbf{k} \times \mathbf{P}; \end{aligned}$$

one has

$$c^2 \frac{1}{\epsilon_0} [\mathbf{k} (\mathbf{k} \cdot \mathbf{E}) - \mathbf{k}^2 \mathbf{E}] = -\mathbf{k} \times \mathbf{B} + \frac{1}{\epsilon_0} \mathbf{k} \times \mathbf{P} + \frac{1}{\epsilon_0} \hat{d} \hat{\epsilon};$$

where we have used the relation $\mathbf{P} = \epsilon_0 \mathbf{E} + \hat{d} \hat{\epsilon}$.

For the transversal component we get

$$c^2 \frac{1}{\epsilon_0} k^2 E_{\perp} = -\mathbf{k} \times \mathbf{B}_{\perp} (1 + \frac{1}{\epsilon_0}) + \frac{1}{\epsilon_0} (\hat{d} \hat{\epsilon})_{\perp};$$

hence,

$$E_{\perp} = \frac{1}{ck} \frac{d}{dt} \mathbf{B}_{\perp};$$

For strain fields associated with phonon propagation, ω and \mathbf{k} are phonon frequency and wavevector and $\omega = k c_s$ so that the transversal component vanishes. Thus, the piezoelectric field accompanying a phonon wave is purely longitudinal and one may introduce the appropriate potential. One has explicitly for the longitudinal component

$$eE_k = \frac{e}{\epsilon_0} \frac{(\hat{d} \hat{\epsilon})_k}{1 + \frac{1}{\epsilon_0}} = -\frac{e}{\epsilon_0} \nabla V(r);$$

where

$$V(r) = \frac{1}{k} \frac{e (\hat{d} \hat{\epsilon})_k}{\epsilon_0 \epsilon_1};$$

Using (7), one finds the strain tensor

$$\epsilon_{ij} = \frac{1}{2} \frac{1}{N} \sum_{s,jk} \frac{\hbar}{2M \omega_s(k)} (\hat{b}_{s,jk} + \hat{b}_{s,-jk}^{\dagger}) [(\hat{e}_{s,jk})_i k_j + (\hat{e}_{s,jk})_j k_i] e^{i\mathbf{k} \cdot \mathbf{r}};$$

In the zincblende structure, one has

$$d_{xyz} = d_{yzx} = d_{zxy} = d; \quad d_{ijk} = d_{ikj};$$

and the other components vanish. Hence

$$(\hat{d} \hat{\epsilon})_k = 2 \frac{d}{k} (k_x k_y z + k_y k_z x + k_z k_x y)$$

and

$$H_{e=h}^{(PE)} = \frac{1}{N} \sum_{s,jk} \frac{\hbar}{2M \omega_s(k)} \frac{de}{\epsilon_0 \epsilon_1} M_s(\hat{k}) (\hat{b}_{k,s} + \hat{b}_{k,s}^{\dagger}) e^{i\mathbf{k} \cdot \mathbf{r}}; \quad (13)$$

where the polarization-dependent geometrical factor is

$$M_s(\hat{k}) = 2 \frac{\hbar}{k} \hat{k}_x \hat{k}_y (\hat{e}_{s,jk})_z + \hat{k}_y \hat{k}_z (\hat{e}_{s,jk})_x + \hat{k}_z \hat{k}_x (\hat{e}_{s,jk})_y;$$

For the choice of the phonon polarizations (l{longitudinal, t1,t2{transversal)

$$\begin{aligned}\hat{e}_{l,k} & \hat{k} = (\cos \cos ; \cos \sin ; \sin); \\ \hat{e}_{t1,k} & = (\sin ; \cos ; 0); \\ \hat{e}_{t2,k} & = (\sin \cos ; \sin \sin ; \cos);\end{aligned}$$

the functions M_s are

$$M_l(;) = \frac{3}{2} \sin 2 \cos \sin 2 ; \quad (14)$$

$$M_{t1}(;) = \sin 2 \cos 2 ; \quad (15)$$

$$M_{t2}(;) = (3 \sin^2 - 1) \cos \sin 2 : \quad (16)$$

Finally, in the second quantization representation,

$$\begin{aligned}H_{e=h}^{(PE)} & = \sum_{nn^0}^X a_n^y a_{n^0}^z \int d^3r \, n(r) V(r) n^0(r) \\ & = \frac{1}{N} \sum_{k;s,nn^0}^X a_n^y a_{n^0}^z f_{e=h,nn^0;s}^{(PE)}(k) b_{k;s} + b_{k;s}^y ;\end{aligned} \quad (17)$$

where

$$f_{e=h,nn^0;s}^{(PE)}(k) = i \frac{s}{2} \frac{h}{V \epsilon_s(k)} \frac{de}{\epsilon_0 \epsilon_1} M_s(\hat{k}) F_{nn^0}(k);$$

with the form factor given by (10).

Note that the LA phonons are coupled to carriers both by the deformation potential and by the piezoelectric coupling, while the TA phonons only by the latter. The piezoelectric coupling results directly from the Coulomb interaction and has exactly opposite value for the electron and the hole. In contrast, there is in general no fixed relation between the values of the deformation potential constants.

Frohlich coupling An LO phonon propagating in a polar medium is accompanied by a polarization field resulting from the relative shifts of the positive and negative ions forming the crystal lattice. Similarly as in the case of piezoelectric coupling, one shows that the resulting electric field is longitudinal and may be associated with a potential. Both the polarization and electric field, and hence the potential, are proportional to the LO phonon displacement. The derivation of the proportionality constant may be found in [8,46]. The resulting interaction energy for the charge carrier at point r is

$$H_{e=h}^{(Fr)} = \frac{1}{N} \sum_k \frac{e}{k} \frac{s}{2v_0} \frac{h}{\epsilon_0} b_{0,k} + b_{0,k}^y e^{ik \cdot r}; \quad (18)$$

where $\epsilon = (\epsilon_1 - \epsilon_s)^{-1}$ is the effective dielectric constant.

In the occupation number representation this reads

$$H_{e=h}^{(Fr)} = \frac{1}{N} \sum_{k,nn^0}^X a_n^y a_{n^0}^z f_{e=h,nn^0}^{(PE)}(k) b_{k;l} + b_{k;l}^y ; \quad (19)$$

where

$$f_{e=h,nn^0}^{(Fr)} = \frac{e}{k} \frac{s}{2v_0} \frac{h}{\epsilon_0} F_{nn^0}(k);$$

Phonon coupling for exciton states Above, we have derived the interaction Hamiltonian in the single-particle basis. However, most of the following deals with excitonic states, i.e. states of con ned electron-hole pairs interacting by Coulomb potentials.

Both carriers forming the exciton couple to phonons according to (9), (17) and (19). If the lowest exciton states are assumed to be approximately of product form, as discussed above, i.e.

$$|i\rangle = a_{e,1}^y a_{h,m}^y |0\rangle;$$

then one gets from (9) the following coupling constants for the deformation potential interaction in the excitonic basis

$$F_{11}^{(DP)}(k) = \frac{\hbar k}{2V_Q} \left(e F_{11}^{(e)}(k) - h F_{11}^{(h)}(k) \right); \quad (20)$$

$$F_{11}^{(DP)}(k) = \frac{\hbar k}{2V_Q} h F_{11}^{(h)}(k); \quad l > 1; \quad (21)$$

It is essential to note that, due to different deformation potential constants e, h , none of these couplings vanishes even if the electron and hole wavefunctions are the same, leading to identical single-particle form factors.

For the Frohlich coupling to LO phonons one has

$$F_{11}^{(Fr)}(k) = \frac{e}{k} \frac{\hbar}{2v_0} F_{11}^{(e)}(k) - F_{11}^{(h)}(k); \quad (22)$$

$$F_{11}^{(Fr)}(k) = \frac{e}{k} \frac{\hbar}{2v_0} F_{11}^{(h)}(k); \quad l > 1; \quad (23)$$

The form of the coupling constants for the piezoelectric interaction is analogous. In the case of Frohlich and piezoelectric coupling, the "diagonal" coupling F_{11} vanishes if the wavefunctions overlap exactly. This results from the fact that both these interaction mechanisms are related directly to the Coulomb interaction between the con ned charge distribution and the phonon-related polarization field. For carriers localized in the same spatial volume but overlapping only partly there will be still some cancellation effect. It is remarkable, however, that even for perfect cancellation of the diagonal coupling, the other contributions F_{1n} , $n > 1$ are not decreased. As we will see, this will lead to additional effects for LO phonons, while in the case of piezoelectric coupling these contributions are negligible due to large energy level spacing compared to the acoustic phonon frequencies.

The spectral properties of the lattice are characterized by the phonon spectral densities

$$R_{nn^0 m m^0}(\omega) = \frac{1}{\hbar^2} n_B(\omega) + \frac{1}{N} \sum_{k,s} F_{nn^0}^{(s)}(k) F_{m m^0}^{(s)}(k) [n_s(k) + n_s(\omega - k)]; \quad (24)$$

where $n_B(\omega) = \frac{1}{e^{\beta\hbar\omega} - 1}$ is the Bose distribution function. These functions depend on the material parameters and system geometry and fully characterize the properties of the lattice subsystem at the level of perturbation treatment discussed in this chapter. As will be seen later, they are one of the two "building blocks" for the perturbative calculation of the phonon effects on a quantum evolution. Here, we will need only a subset of these functions, $R_1(\omega) = R_{11,11}(\omega)$.

Let us consider the functions $R_1^{(LA)}(\omega)$, corresponding to the LA phonons. Here the total coupling $F_{11}^{(LA)}$ contains both DP and PE contributions. However, under reasonable symmetry assumptions the form factors may be chosen either real or purely imaginary [see e.g. the explicit form for the harmonic con nement, Eq. (12)], while the coefficients in (9) and (17) are purely real and purely

imaginary, respectively. Thus, the spectral densities split into two independent contributions. Substituting (20,21) into (24) and performing the summation over k in the usual continuum limit

$$\sum_k \rightarrow \frac{NV}{(2\pi)^2} \int d^3k;$$

one obtains

$$R_1^{(DP)}(\omega) = R_{DP} \{ n_B(\omega) + 1 \} f_1(\omega); \quad (25)$$

where

$$R_{DP} = \frac{(e \hbar)^2}{4 \pi^2 \hbar \epsilon_1^5}$$

and $f_1(\omega)$ are certain functions that depend on the wavefunction geometry, having the property $f_1(0) = 1$ and $f_1(\infty) = 0$, $1 > 1$. A similar procedure leads to an analogous result for the piezoelectric contribution from LA phonons.

In the case of dispersionless LO phonons $\omega_o(k) = \omega_o$ and the spectral densities are

$$\begin{aligned} R_1^{(Fr)}(\omega) &= R_{Fr} n_B(\omega) + 1 \{ f_1(\omega - \omega_o) + f_1(\omega + \omega_o) \} \\ R_1^{(Fr)}(\omega) &= R_{Fr}^0 n_B(\omega) + 1 \{ f_1(\omega - \omega_o) + f_1(\omega + \omega_o) \} \end{aligned}$$

where

$$R_{Fr} = \frac{3 e^2}{8 \pi^2 \epsilon_o L} \frac{(\epsilon_e^2 - \epsilon_h^2)^2}{16 L^4}; \quad R_{Fr}^0 = \frac{e^2}{8 \pi^2 \epsilon_o L^3};$$

and $\epsilon_{(00)} = 1$, $\epsilon_{(01)} = 1/4$, $\epsilon_{(02)} = 3/32$, $\epsilon_{10} = 3/16$. Here we numbered the states by $(N; M)$, where M is the total angular momentum and N is another quantum number, and introduced the averaged carrier localization $L^2 = (\epsilon_e^2 + \epsilon_h^2)/2$, where ϵ_e, ϵ_h correspond to ϵ_e in Eq. (11) for electrons and holes, respectively, and $\epsilon_e^2 - \epsilon_h^2 = L^2$.

4 Decoherence of carrier states by a dressing process

Any optical experiment or optical control of carrier states in a quantum dot is based on the coupling between the carriers and the electric field of the electromagnetic wave. By using high-power laser pulses this coupling can be made strong, leading to fast excitation of confined excitons. However, this coupling involves pure electronic degrees of freedom, inducing only carrier transitions which must then be followed by lattice relaxation to the potential minimum corresponding to the newly created charge state. In the case of the optical exciton creation, the initial lattice configuration corresponds to zero polarization field and zero deformation, while the eigenstate of the interacting system involves some lattice polarization (LO phonon field) and some deformation (LA phonon field). Thus, the process of the lattice relaxation may be viewed as the formation of the phonon dressing around the confined exciton. The lattice relaxation process, accompanied by a non-zero probability of phonon emission, only takes place if the result of a control pulse is a one-exciton state. Hence, if the pulse creates a superposition, the lattice dynamics is different for the two components of the superposition state, leading to entanglement between the carrier and lattice degrees of freedom and to decoherence. Physically, detection of a phonon carrying out the excess energy during the lattice relaxation process reduces the superposition of carrier states to the one-exciton state, since the other state (empty dot) is never accompanied by the lattice relaxation. It should be kept in mind, however, that unlike in the phonon-assisted carrier relaxation processes, the average number of phonons emitted during the dressing is much less than one (in the weak coupling case) and even in the limit of $t \rightarrow \infty$ the emission probability is below 1, leading only to partial loss of the carrier coherence [29,30].

In this section we discuss the carrier-phonon kinetics after an ultra-fast excitation from the point of view of decoherence and "information leakage" from the carrier subsystem [30] (see [29,31,32] for an exhaustive discussion from the point of view of the optical properties).

We consider a quantum dot in which an exciton is created by a very short laser pulse. We assume that the pulse is much shorter than the periods of the phonons but long enough to ensure spectral overlap only with one (ground-state) exciton transition. We allow, however, for the existence of dark states of energy much lower than the closest bright state, as discussed in the section 2. In accordance with the discussion in section 3, we include in the interaction Hamiltonian (3) the deformation potential coupling to LA phonons and Frohlich coupling to LO phonons.

In order to quantify the quality of a manipulation on the quantum state from the point of view of the desired goal, one defines the fidelity as the overlap between the desired final state obtained from the initial state $|j_0\rangle$ by the unperturbed evolution U_C and the actual state described by the reduced density matrix of the carrier subsystem $\rho(t)$,

$$F = 1 - \langle \rho(t) | U_C^\dagger(t) | j_0 \rangle \langle j_0 | U_C(t) | \rho(t) \rangle = 1 - \langle \rho(t) | U_C^\dagger(t) | j_0 \rangle \langle j_0 | U_C(t) | \rho(t) \rangle; \quad (26)$$

where $\langle \cdot \rangle$ denotes thermal average over the initial lattice states. If the initial carrier state is the vacuum $|j_0\rangle$ and the operation, performed at $t = 0$, is an ultra-fast rotation by the angle θ on the Bloch sphere corresponding to the $|j_0\rangle$ and $|j_1\rangle$ states than the unperturbed state for $t > 0$ is

$$|j(t)\rangle = U_C(t) |j_0\rangle = \cos \frac{\theta}{2} |j_0\rangle - i e^{iE_1 t} \sin \frac{\theta}{2} |j_1\rangle; \quad (27)$$

Let us calculate the actual state, including phonon perturbations, in this ultrafast limit. The diagonal elements of the density matrix remain constant, since phonon processes cannot change the excitonic occupations,

$$\rho_{00} = \cos^2 \frac{\theta}{2}; \quad \rho_{11} = \sin^2 \frac{\theta}{2};$$

while for the non-diagonal ones one finds

$$\rho_{10}(t) = \text{Tr} [\rho(t) |j_1\rangle \langle j_0|] = \frac{1}{2} i \sin \theta e^{-iE_1 t}; \quad (28)$$

where we have substituted $\rho(t) = |j(t)\rangle \langle j(t)|$ with $|j(t)\rangle$ given by (27), and defined the correlation function

$$G(t) = \langle U^\dagger(t) |j_1\rangle \langle j_0| U(t) |j_0\rangle \langle j_1|; \quad (29)$$

where $U(t)$ is the evolution operator for the total interacting system. Using the definition (26), the fidelity loss may be expressed as

$$F(t) = 1 - \frac{1}{2} \sin^2 \theta \text{Re} G(t) e^{iE_1 t}; \quad (29)$$

In order to find the correlation function we describe the carrier-phonon kinetics after an abrupt excitation using the basis of perturbative eigenstates of the Hamiltonian $H = H_C + H_{int}$ [20,14]. Thus, we introduce the new states and operators

$$|j_i\rangle = e^S |j_i\rangle; \quad b_k = e^S b_k e^{-S};$$

corresponding to dressed particles. The system Hamiltonian expressed in terms of these operators is diagonal up to second-order corrections if the anti-hermitian operator S is chosen as

$$S = \sum_{n \neq 0} \sum_{k,s} \frac{1}{\epsilon_n} \langle n | H_{int} | 0 \rangle b_{k,s}^\dagger b_{k,s}^{(n)}; \quad (30)$$

where

$$F_{nn^0}^{(s)}(k) = \frac{F_{nn^0}^{(s)}(k)}{E_{n^0} - E_n + \hbar \omega_s(k)};$$

and $F_{nn^0}^{(s)}$ are given by (20-23). Therefore, the evolution of these new states and operators is free,

$$|n\rangle(t) = |n\rangle e^{-i\frac{E_n}{\hbar}t}; \quad |s;k\rangle(t) = |s;k\rangle e^{-i\omega_s(k)t};$$

where E_n is the exciton energy including corrections resulting from the interaction.

To the lowest order, the creation operator for the ground exciton state may now be written as

$$\begin{aligned} |n\rangle &= e^S |n\rangle e^{-S} \\ &= \left(1 - \frac{1}{2N} \sum_{n;s;k} j_{0n}^{(s)}(k) j_{s;k}^2 (2n_{s;k} + 1)\right) |n\rangle \\ &\quad + \frac{1}{N} \sum_{n;s;k} j_{0n}^{(s)}(k) |n\rangle j_{s;k} + |s;k\rangle : \end{aligned}$$

Using these formulae, it is easy to write down the correlation function

$$\begin{aligned} G(t) &= \left(1 - \frac{1}{N} \sum_{n;s;k} j_{0n}^{(s)}(k) j_{s;k}^2 (2n_{s;k} + 1)\right) e^{-i\frac{E_1}{\hbar}t} \\ &\quad + \frac{1}{N} \sum_{n;s;k} n_{s;k} j_{0n}^{(s)}(k) j_{s;k}^2 e^{-i(E_n - \hbar \omega_s(k))t} \\ &\quad + \frac{1}{N} \sum_{n;s;k} (n_{s;k} + 1) j_{n0}^{(s)}(k) j_{s;k}^2 e^{-i(E_n - \hbar \omega_s(k))t}; \end{aligned}$$

where $n_{s;k}$ are the thermal occupation numbers for phonon modes. It should be noted that the perturbative treatment is valid only when the above correlation function remains close to one. For a fixed strength of interaction this requires a low enough temperature (in practice, for a typical InAs/GaAs dot, this means $T < 100$ K).

In order to explain the time evolution of this function, let us remember that the functions $F_{nn^0}^{(s)}(k)$ contain the form factors (10), effectively selecting a certain wavenumber range $k_0^{(s)} - \frac{1}{2} k^{(s)}$, centered around $k_0^{(s)}$ for each branch of phonons ($k^{(s)} = l$, where l is the dot size). This corresponds to a certain frequency range $\omega_0^{(s)} - \frac{1}{2} \omega^{(s)}$, around a central frequency $\omega_0^{(s)}$. The phases that enter in the summation in (30) at the time t spread effectively over the angle range $\omega_0^{(s)}t - \frac{1}{2} \omega^{(s)}t$. When this phase spreading reaches 2π , i.e. for $t = \frac{2\pi}{\omega^{(s)}}$, the last two terms in (30) become small. The asymptotic value of the corresponding error is

$$= \frac{1}{2} \sin^2 \frac{1}{N} \sum_{k;n;s} j_{0n}^{(s)}(k) j_{s;k}^2 (2n_{s;k} + 1):$$

In the case of acoustical phonons this value critically depends on temperature (Fig. 1a). The decoherence time depends on the phonon dispersion (the frequency range $\omega^{(s)}$) and weakly evolves with temperature. For the acoustical phonons, $\omega = 2\pi \times 10^{12}$ ps (Fig. 1a). For the nearly dispersionless optical phonons, the dynamics is dominated by slowly vanishing coherent phonon beats (Fig. 1b,c). However, in order to excite these oscillations one needs pulses shorter than LO phonon periods, i.e. of durations < 10 fs. Moreover, it is known that the anharmonic LO-TO interaction [48,49] (not included in the present description) acts on much shorter timescales and may be expected to considerably shorten this time.

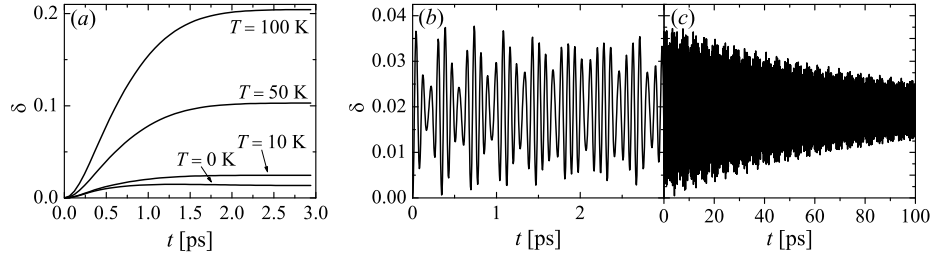


Figure 1: Dressing-induced decoherence of the exciton due to LA phonons (a) and due to LO phonons: oscillations with LO phonon frequency (b) decay on a very long timescale (c) (anharmonic effects are not included). Four lowest exciton states calculated by numerical diagonalization [30] were taken into account.

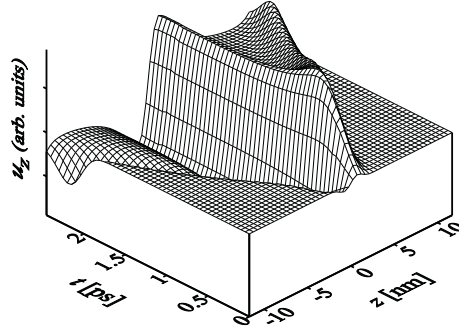


Figure 2: Time evolution of the mean lattice deformation (acoustic phonons) at the dot axis ($x = y = 0$). The time-independent deformation, corresponding to the coherent phonon dressing, is formed around $z = 0$ (i.e. in the dot area) within ~ 1 ps. This is accompanied by emission of a phonon packet carrying away the excess energy at the speed of sound, seen on the plot as the ridge and the valley with growing distance from the dot.

It is possible to see directly that the described process consists in the formation of a coherent (i.e. with non-vanishing mean displacement) phonon field corresponding to the classical lattice deformation around the confined charge. Let us consider the mean lattice displacement corresponding to the branches at the point r after time t after rapid creation of an exciton. Using (7) and transforming to the dressed basis one obtains in the lowest order

$$\langle \hat{u}_s(r;t) \rangle_{i_T} = \frac{1}{N} \sum_k \frac{\hbar}{2\omega_s(k)} e^{ik \cdot r} \text{Re} \left[\sum_s \frac{\hbar}{2\omega_s(k)} e^{i\omega_s(k)t} \right] :$$

After a sufficiently long time the oscillating term averages to zero (around $r = 0$) and a time-independent displacement field is formed. The Fig. 2 shows the mean lattice deformation due to the deformation potential coupling on the dot axis, $r = (0;0;z)$, at various instances of time. A simple and intuitive picture emerges: formation of the lattice deformation, corresponding to the displaced equilibrium, is accompanied by emitting a phonon packet that carries the excess energy away from the dot with the speed of sound. It is clear that as soon as these wavepackets leave the volume of the dot, some information about the carrier state is carried into the outside world. Also, since the only controlled interaction is that with the confined carriers, once the phonons have been radiated out the reversibility is lost.

We have shown that the carrier-phonon coupling leads to entanglement of the carrier system and the surrounding lattice. This, in turn, reduces the degree of coherence of the carrier subsystem. This decoherence is related to the spontaneous relaxation of the lattice to the new equilibrium defined by the carrier-phonon interaction and results from the non-adiabaticity of carrier evolution with respect

to the lattice response times. It may be expected that for a slow enough evolution most of the lattice modes will follow adiabatically, thus creating the coherent dressing cloud in a reversible way. In the following sections we derive the formalism suitable for the description of the carrier-phonon kinetics and apply it to a few problems.

5 Evolution of the density matrix for a driven carrier-phonon system

In this section we derive the equations for the reduced density matrix of the carrier subsystem in the leading order in the phonon coupling, assuming that the unperturbed evolution is known. This somewhat lengthy and technical derivation yields very simple and intuitive formulas that may be easily applied to a range of problems to be discussed in the subsequent sections.

We will consider a system composed of charge carriers (electrons and holes), localized in one or more quantum dots, driven externally and interacting with phonons, as described by the Hamiltonian (1). As already mentioned, the evolution of the carrier subsystem is generated by the (time dependent) Hamiltonian H_C , describing the properties of the system itself as well as its coupling to driving fields. In this chapter, we deal only with optical driving (although not necessarily via direct excitation of dipole-allowed transitions), but other types of external fields may be treated on the same footing. The evolution of the phonon subsystem (reservoir) is described by the Hamiltonian H_{ph} [Eq. (2)]. We will restrict the discussion to the free phonon evolution, neglecting anharmonicity effects. The evolution operator for the driven carrier subsystem and free phonon modes, without carrier-phonon interaction is

$$U_0(t) = U_C(t) e^{iH_{ph}(t-s)};$$

where $U_C(t)$ is the operator for unperturbed evolution of the carrier subsystem (we suppress the initial time in $U(t;s)$).

The carrier-phonon coupling is described by the interaction Hamiltonian (3) which may be written in the form

$$V = \sum_{nn^0} S_{nn^0} R_{nn^0}; \quad (30)$$

where $n; n^0$ run over the carrier subsystem states, S_{nn^0} (possibly time-dependent) act in the Hilbert space of the carrier subsystem while the time-independent R_{nn^0} affect only the environment. It is convenient to allow non-Hermitian operators S_{nn^0} and R_{nn^0} ; however, we demand the symmetry relation

$$S_{nn^0}^\dagger = S_{n^0n}; \quad R_{nn^0}^\dagger = R_{n^0n} \quad (31)$$

which guarantees hermiticity of the Hamiltonian (30) and is also explicitly satisfied by (3).

We will assume that at the initial times the system is in the product state

$$\rho(s) = |j_0\rangle \langle j_0| \otimes \rho_T; \quad (32)$$

where $|j_0\rangle$ is a certain state of the carrier subsystem and ρ_T is the thermal equilibrium distribution of phonon modes. Physically, such an assumption is usually reasonable due to the existence of two distinct time scales: the long one for the carrier decoherence (e.g. 1 ns ground state exciton lifetime [28,50]) and the short one for the reservoir relaxation (1 ps dressing time [28,30]).

The starting point is the evolution equation for the density matrix of the total system in the interaction picture with respect to the externally driven evolution U_0 , in the second order Born approximation with respect to the carrier-phonon interaction [51]

$$\rho(t) = \rho(s) + \frac{1}{i\hbar} \int_s^t ds' [V(s'); \rho(s')] - \frac{1}{\hbar^2} \int_s^t ds' \int_s^{s'} ds'' [V(s'); [V(s''); \rho(s)]]; \quad (33)$$

where

$$\% (t) = U_0^Y(t) \% (t) U_0(t); \quad V(t) = U_0^Y(t) V U_0(t)$$

(it should be kept in mind that V may depend on time itself).

The reduced density matrix of the carrier subsystem at time t is

$$\rho(t) = U_C(t) \rho(0) U_C^Y(t); \quad \tilde{\rho}(t) = \text{Tr}_R \rho(t);$$

where the trace is taken over the reservoir degrees of freedom. The first (zeroth order) term in (33) obviously gives rise to

$$\rho^{(0)}(t) = U_C(t) \rho(0) U_C^Y(t) = \rho(0) U_C(t) U_C^Y(t); \quad (34)$$

The second term vanishes, since it contains the thermal average of an odd number of phonons. The third (second order) term describes the leading phonon correction to the dynamics of the carrier subsystem,

$$\rho^{(2)}(t) = \frac{1}{h^2} \int_0^t ds \int_0^s ds' \text{Tr}_R [V^{(0)}; [V^{(0)}; \rho(s)]]; \quad (35)$$

First of the four terms resulting from expanding the commutators in (35) is

$$(I) = Q_t \rho(0) \dot{\rho}(0)$$

where

$$Q_t = \frac{1}{h^2} \sum_{nn^0 mm^0} X_{nn^0} X_{mm^0} \int_0^t ds \int_0^s ds' \text{Tr}_{nn^0} (S_{nn^0}^{(0)} S_{mm^0}^{(0)} h R_{nn^0}^{(0)} R_{mm^0}^{(0)}) \rho(0); \quad (36)$$

The operators S and R are transformed into the interaction picture in the usual way

$$S_{nn^0}(t) = U_0^Y(t) S_{nn^0} U_0(t); \quad R_{nn^0}(t) = U_0^Y(t) R_{nn^0} U_0(t)$$

and $\langle \hat{O} \rangle = \text{Tr}_R [\hat{O} \rho_T]$ denotes the thermal average (obviously $[U_0(t); \rho_T] = 0$).

The second term is

$$(II) = \frac{1}{h^2} \sum_{nn^0 mm^0} X_{nn^0} X_{mm^0} \int_0^t ds \int_0^s ds' \text{Tr}_{nn^0} [\rho(0) \dot{S}_{nn^0}^{(0)} S_{mm^0}^{(0)} h R_{mm^0}^{(0)} R_{nn^0}^{(0)}] \rho(0);$$

Using the symmetry relations (31) one has

$$h R_{mm^0}^{(0)} R_{nn^0}^{(0)} = h R_{nn^0}^{(0)} R_{mm^0}^{(0)}; \quad S_{mm^0}^{(0)} S_{nn^0}^{(0)} = S_{nn^0}^{(0)} S_{mm^0}^{(0)}; \quad (37)$$

hence this term may be written as

$$(II) = \rho(0) \dot{Q}_t \rho(0)$$

In a similar manner, using the symmetries (31), the two other terms may be combined to

$$(III) + (IV) = \hat{Q}_t [\rho(0) \dot{\rho}(0)];$$

where

$$\hat{Q}_t = \frac{1}{h^2} \sum_{nn^0 mm^0} X_{nn^0} X_{mm^0} \int_0^t ds \int_0^s ds' \text{Tr}_{nn^0} (S_{nn^0}^{(0)} S_{mm^0}^{(0)} h R_{mm^0}^{(0)} R_{nn^0}^{(0)}) \rho(0); \quad (38)$$

In terms of the new Hermitian operators

$$A_t = Q_t + Q_t^Y; \quad h_t = \frac{1}{2i} (Q_t - Q_t^Y); \quad (39)$$

the density matrix at the final time t (34,35) may be written as

$$\rho(t) = U_C(t) \rho(0) U_C^Y(t) + i [h_t; \rho(0) \dot{\rho}(0)] + \hat{Q}_t [\rho(0) \dot{\rho}(0)] U_C^Y(t); \quad (40)$$

The first term is a hamiltonian correction which does not lead to irreversible effects and, in principle, may be compensated for by an appropriate modification of the control Hamiltonian H_c . The other two terms describe processes of entangling the system with the reservoir, leading to the loss of coherence of the carrier state.

Let us introduce the spectral density of the reservoir,

$$R_{nn^0 m m^0}(\omega) = \frac{1}{2\hbar^2} \int_{-\infty}^{\infty} dt R_{nn^0}(t) R_{m m^0}^\dagger e^{i\omega t}; \quad (41)$$

If the operators R_{nn^0} are linear combinations of freely evolving bosonic modes (only this case will be considered in this chapter),

$$R_{nn^0} = R_{n^0 n}^\dagger = \frac{1}{N} \sum_k F_{nn^0}(k) b_k + b_k^\dagger; \quad (42)$$

with $F_{nn^0}(k) = F_{n^0 n}(k)$ (branch index implicit in k), then (41) coincides with (24).

With the help of (41) one may write

$$\hat{\chi}_t = \sum_{nn^0 m m^0} \sum_{\omega} \int_{-\infty}^{\infty} d\omega' R_{nn^0 m m^0}(\omega') Y_{m m^0}(\omega') Y_{n^0 n}^\dagger(\omega) \quad (43)$$

where the frequency-dependent operators have been introduced,

$$Y_{nn^0}(\omega) = \int_{-\infty}^{\infty} dt S_{nn^0}(\omega) e^{i\omega t}; \quad (44)$$

Using (41) one has also

$$Q_t = \sum_{nn^0 m m^0} \sum_{\omega} \int_{-\infty}^{\infty} dt \int_{-\infty}^{\infty} dt' d\omega' d\omega'' (\omega'' - \omega') S_{nn^0}(\omega') S_{m m^0}(\omega'') R_{nn^0 m m^0}(\omega) e^{i\omega'' t} e^{-i\omega' t};$$

Next, representing the Heaviside function as

$$\theta(t) = e^{i\omega t} \int_{-\infty}^{\infty} d\omega' \frac{e^{-i\omega' t}}{i(\omega' - \omega) + i0};$$

we write

$$\begin{aligned} Q_t &= \sum_{nn^0 m m^0} \sum_{\omega} \int_{-\infty}^{\infty} d\omega' R_{nn^0 m m^0}(\omega') \int_{-\infty}^{\infty} d\omega'' \frac{Y_{n^0 n}^\dagger(\omega'') Y_{m m^0}(\omega'')}{2i(\omega'' - \omega) + i0} \\ &= \sum_{nn^0 m m^0} \int_{-\infty}^{\infty} d\omega' R_{nn^0 m m^0}(\omega') \int_{-\infty}^{\infty} d\omega'' \frac{Y_{n^0 n}^\dagger(\omega'') Y_{m m^0}(\omega'')}{2i(\omega'' - \omega) + i0} + P \frac{1}{i(\omega - \omega)}; \end{aligned}$$

where P denotes the principal value.

Hence, the two Hermitian operators defined in (39) take the form

$$A_t = \sum_{nn^0 m m^0} \sum_{\omega} \int_{-\infty}^{\infty} d\omega' R_{nn^0 m m^0}(\omega') Y_{n^0 n}^\dagger(\omega') Y_{m m^0}(\omega') \quad (45)$$

and

$$h_t = \sum_{nn^0 m m^0} \sum_{\omega} \int_{-\infty}^{\infty} d\omega' R_{nn^0 m m^0}(\omega') P \int_{-\infty}^{\infty} d\omega'' \frac{Y_{n^0 n}^\dagger(\omega'') Y_{m m^0}(\omega'')}{2i(\omega'' - \omega)}; \quad (46)$$

where we have used the relation

$$R_{nn^0, m m^0}(\mathbf{l}) = R_{m^0 m, n n^0}(\mathbf{l});$$

resulting from the definition (41) and the symmetry relation (37).

Using the definition of the density (26) and the Master equation (40), the error may be written in a general case as

$$= \langle \mathbf{h}_0 | \hat{\mathbf{A}}_t | \mathbf{j}_0 \rangle \langle \mathbf{j}_0 | \hat{\mathbf{h}}_0 | \mathbf{j}_0 \rangle : \quad \begin{matrix} D \\ E \end{matrix}$$

It should be noted that the unitary correction generated by \mathbf{h}_t does not contribute to the error at this order.

Using the definitions (38,45) this may be further transformed to

$$= \sum_{nn^0, m m^0} \langle \mathbf{l} | R_{nn^0, m m^0}(\mathbf{l}) \rangle \langle \mathbf{j}_0 | \mathbf{Y}_{n n^0}^Y(\mathbf{l}) P^\perp \mathbf{Y}_{m m^0}(\mathbf{l}) | \mathbf{j}_0 \rangle ; \quad (47)$$

where P^\perp is the projector on the orthogonal complement of \mathbf{j}_0 in the carrier space.

6 Phonon-induced damping of Rabi oscillations

Introduction. Observation of Rabi oscillations of charge degrees of freedom confined in quantum dots [26] is believed to be a fundamental step towards quantum control of these systems. However, the coherent dynamics of the confined carrier states is very sensitive to any interaction with the macroscopic number of degrees of freedom of the outside world. In fact, so far it has always turned out that experimentally observable Rabi oscillations deviate from the ideal ones, the discrepancy being larger for stronger pulses. In principle, this might also be explained by experimental conditions or environmental perturbation: scattering by weakly localized excitons around an interface fluctuation QD (further confined by increasing decay for stronger pulses) [2], tunneling to leads in the photodiode structure (on 10 ps timescale) [4], or dipole moment distribution in the QD ensemble [28].

One might believe that all the perturbation comes from sources that may be removed or minimized by technology improvement and by optimizing the experimental conditions and hence produce no fundamental obstacle to arbitrarily perfect quantum control over the excitonic states. However, in every case the QDs are inherently coupled to the surrounding crystal lattice. The recent theoretical study [33] on optical Rabi-opping of excitons in QDs driven by finite-length optical pulses in the presence of the lattice reservoir shows that exponential damping models fail to correctly describe the system kinetics. The appropriate quantum-kinetic description yields much less damping, especially for long pulses. It turns out that the lowest "quality" of the Rabi oscillation is obtained for pulse durations of a few ps, while for longer durations the damping is again decreased.

In this section we discuss both qualitative and quantitative explanation [34] of the mechanism leading to the phonon-induced damping reported in the theoretical and experimental studies. We show that the carrier-phonon interaction responsible for the damping of the oscillations has a resonant character: While in the linear limit the system response depends only on the spectral decomposition of the pulse, the situation is different when a strong pulse induces an oscillating charge distribution in the system. In a semi-classical picture, this would act as a driving force for the lattice dynamics. If the induced carrier dynamics is much faster than phonon oscillations the lattice has no time to react until the optical excitation is done. The subsequent dynamics will lead to exciton dressing, accompanied by emission of phonon packets, and will partly destroy coherence of superposition states [28{31] but cannot change the exciton occupation number. In the opposite limit, the carrier dynamics is slow enough for the lattice to follow adiabatically. The optical excitation may then be stopped at any stage without any lattice relaxation incurred, hence with no coherence loss.

The intermediate case corresponds to modifying the charge distribution in the QD with frequencies resonant with the lattice modes which leads to increased interaction with phonons and to decrease of the carrier coherence (see Ref. [52] for a simple, single-mode model).

The formalism In one version of the experiment [2,4,5] one measures the average occupation of the exciton ground state, $\langle |j\rangle\langle j| \rangle$, after a resonantly coupled pulse of fixed length but variable amplitude, starting with the system in the ground state $|j\rangle$. According to (27), in the ideal case the final occupation should vary as

$$\langle |j\rangle\langle j| \rangle_{\text{ideal}} = \sin^2 \frac{1}{2} \theta;$$

where

$$\theta = \theta(1) = \int_0^Z dt \sqrt{1 - \sin^2 \theta(t)};$$

is the total pulse area. Within our formalism, the final occupation of the exciton state is given directly by the appropriate diagonal element of (40), once the spectral integrals entering in (38) and (45) for a given pulse are calculated.

The interaction Hamiltonian has the form (3), with the coupling constants (20-23). Hence, $S_{nn^0} = \delta_{nn^0}$, $n = 1, 2, \dots$ and, using the explicit form of the evolution operator (27), the operators (44) may be written in the form ($n, n^0 > 1$; we integrate by parts in order to extract the oscillatory contributions)

$$Y_{11} = \langle |j\rangle\langle j| \rangle = \langle |j\rangle\langle j| \rangle_0 \frac{1}{2!} \int_0^Z dt \sin^2 \theta(t) K_s^{(1)}(t) + \langle |j\rangle\langle j| \rangle_0 \frac{i}{2!} \int_0^Z dt \cos \theta(t) e^{i\theta(t)} K_c^{(1)}(t) + \langle |j\rangle\langle j| \rangle_0 \frac{1}{2!} \int_0^Z dt e^{i\theta(t)} e^{i\theta(t)};$$

$$Y_{n1} = \langle |j\rangle\langle j| \rangle \frac{1}{(1+n)!} e^{i\theta(t)} \sin \frac{1}{2} \theta(t) K_s^{(1=2)}(t) + \langle |j\rangle\langle j| \rangle \frac{i}{(1+n)!} e^{i\theta(t)} \cos \frac{1}{2} \theta(t) e^{i\theta(t)} K_c^{(1=2)}(t) + \langle |j\rangle\langle j| \rangle \frac{1}{(1+n)!} e^{i\theta(t)} e^{i\theta(t)};$$

$$Y_{nn^0} = \langle |j\rangle\langle j| \rangle \frac{i}{(1+n)!} e^{i\theta(t)} e^{i\theta(t)} e^{i\theta(t)} K_s^{(1=2)}(t) + \langle |j\rangle\langle j| \rangle \frac{1}{(1+n)!} e^{i\theta(t)} e^{i\theta(t)} e^{i\theta(t)} K_c^{(1=2)}(t) + \langle |j\rangle\langle j| \rangle \frac{1}{(1+n)!} e^{i\theta(t)} e^{i\theta(t)} e^{i\theta(t)};$$

where $\theta = \theta(1)$ is the total rotation angle and

$$K_s^{(1)}(t) = \int_0^Z dt e^{i\theta(t)} \frac{d}{dt} \sin \theta(t); K_c^{(1)}(t) = \int_0^Z dt e^{i\theta(t)} \frac{d}{dt} \cos \theta(t);$$

In the limit of $s \rightarrow 1$, $t \rightarrow 1$ (i.e. measurement after sufficiently long time compared to the reservoir memory), the functions (51) actually depend only on θ_p , where θ_p is the pulse duration.

Since the unperturbed evolution operator (27) has a block-diagonal structure and conserves the subspace spanned by $|j\rangle$ and $|j\rangle$, the value of $\rho_{11}(t)$ is determined by the matrix elements of $\tilde{\rho}(t)$ between these two states, while ρ_{11} for $l > 1$ has the same form as in the interaction picture. Retaining only non-vanishing contributions, these matrix elements are, from (40), with $j_0 = |j\rangle$,

$$\rho_{00} = \frac{1}{Z} \int_0^Z dt R_1(t) \langle |j\rangle\langle j| \rangle; \rho_{01} = \frac{1}{Z} \int_0^Z dt R_1(t) \langle |j\rangle\langle j| \rangle;$$

$$\rho_{11} = \frac{1}{2} \langle |j\rangle\langle j| \rangle \rho_{11} \langle |j\rangle\langle j| \rangle + \frac{1}{2} \langle |j\rangle\langle j| \rangle \rho_{11} \langle |j\rangle\langle j| \rangle + \frac{1}{2} \langle |j\rangle\langle j| \rangle \rho_{11} \langle |j\rangle\langle j| \rangle$$

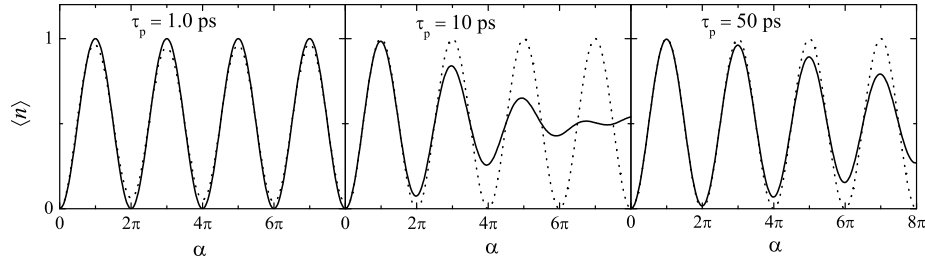


Figure 4: Pulse-area-dependent Rabi oscillations for various pulse durations τ_p as shown in the figure, for $T = 10$ K (α is the rotation angle on the Bloch sphere). Dotted line shows unperturbed oscillations. The wavefunction localization widths are $l_e = 4.9$ nm, $l_h = 4.0$ nm, $l_z = 1$ nm.

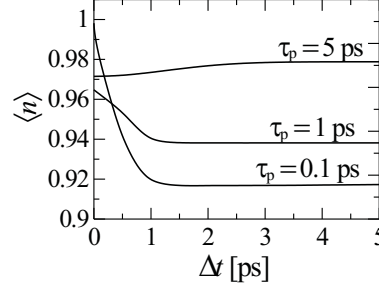


Figure 5: The final QD occupation after two $\pi/2$ pulses separated by time interval t for pulse durations as shown.

of the optically controlled exciton dynamics for $\tau_p = 1$ ps (the characteristics for other durations is easily obtained by scaling). According to (55)-(57), the overlap of these spectral characteristics with the phonon spectral density gives the perturbation of the coherent carrier dynamics.

All the spectral densities $R_l(\omega)$ contain contributions from all the phonon branches and all carrier-phonon coupling channels. For the LO phonons, they are peaked at $\omega = \omega_l + \omega_c$ (at low temperatures). One should note that the denominators ω and $\omega + \omega_l$ are of the same order of magnitude, while the strength of the spectral density is much stronger for $l = 2$ because of the charge cancellation effect decreasing the ground-state contribution. Therefore, the response from the higher states is stronger. Physically, it corresponds to phonon-assisted excitation of a dark state. Obviously, the spectral functions $S_{ac}(\omega)$ must extend to this high frequency sector.

For acoustical phonons, in contrast, the spectral density are concentrated at low frequencies, so that the denominators $(\omega + \omega_l)^2$ for $l = 2$ are at least two orders of magnitude higher than the typical frequency ω^2 appearing in the $l = 1$ term. Therefore, the contribution from the acoustic phonons is restricted to the ground state term. For the piezoelectric coupling, this term is strongly reduced by the charge cancellation; therefore, the effect of this coupling on the exciton coherence may be neglected as long as the electron and hole densities for the excitonic ground state overlap.

Damping due to the LA phonons. Let us first discuss the case of relatively long pulses (picosecond durations) and discuss the contributions from the LA phonons only, neglecting the existence of the higher states. The results of such calculations is shown in Fig. 4 for Gaussian pulses [τ_p is the full width at half maximum of the pulse envelope $f(t)$].

The oscillations are almost perfect for very short pulses ($\tau_p = 1$ ps), then lose their quality for longer pulse durations ($\tau_p = 10$ ps). Although this might be expected from any simple decoherence model, the striking feature is that the effect dramatically grows for higher oscillations, despite the fact that the whole process has exactly constant duration. Even more surprising is the improvement of the quality of oscillations for long pulses ($\tau_p = 50$ ps) where, in addition, the first oscillation is nearly

perfect.

For growing number of rotations n , the nonlinear pulse spectrum $S_a(\omega)$ develops a series of maxima of increasing strength (Fig. 3a,b,c). The position of the last and highest maximum corresponds approximately to $2n = \omega_p$, in accordance with the semiclassical resonance concept. However, spectral components are also present at all the frequencies $2n = \omega_p$, $n^0 < n$, which is due to the turning on/off of the pulse. It is interesting to note that for high n , the low-frequency part of $S_a(\omega)$ does not evolve with n (Fig. 3d). It is now clear that there are two ways of minimizing the overlap: either the pulse must be so short that all the maxima of $S_a(\omega)$ are pushed to the right into the exponentially vanishing tail of the reservoir spectral density $R(\omega)$, or the pulse must be very long, to "squeeze" the spectral function near $\omega = 0$ and thus reduce its area. In the latter case, the maxima developing with growing number of oscillations will eventually overlap with $R(\omega)$ destroying the coherence.

Although it might seem that speeding up the process is the preferred solution, it is clear that this works only because no high frequency features are included into the present model. In reality, speeding up the dynamics is limited e.g. by the presence of excited states and non-adiabatically enhanced LO phonon coupling (see below). Moreover, it turns out that the resulting dynamics is actually not fully coherent. It has been shown [31] that superposition of states created by an ultra-short $\tau_p = 2$ ps pulse becomes corrupted, preventing a second pulse (after some delay time t) from generating the final state of $n_{fi} = 1$ with unit efficiency. In order to prove the fully coherent character of carrier dynamics it is necessary to demonstrate the stability of the intermediate state in a two-pulse experiment. The simulations of such an experiment are shown in Fig. 5. A short pulse ($\tau_p = 0.1$ ps) creates a superposition of bare states (surrounded by non-distorted lattice) which then decohere due to dressing processes [29,14]. As a result, the exciton cannot be created by the second pulse with unit probability [31]. For a longer pulse ($\tau_p = 1$ ps), the lattice partly manages to follow the evolution of charge distribution during the optical operation and the destructive effect is smaller. Finally, if the carrier dynamics is slow compared to the lattice response times ($\tau_p = 10$ ps), the lattice distortion follows adiabatically the changes in the charge distribution and the superposition created by the first pulse is an eigenstate of the interacting carrier-lattice system, hence does not undergo any decoherence and the final effect is the same for any delay time (its quality limited by decoherence effects during pulsing). In fact, splitting the pulse into two corresponds to slowing down the carrier dynamics which, in the absence of decoherence during delay time, improves the quality of the final state, as seen in Fig 5.

Effects of LO phonons. The above discussion focused on the relatively long pulse durations when the contribution from the LO phonons is negligible. However, an interesting manifestation of the resonance effect may be observed for sub-picosecond pulses, when the excitation of longitudinal optical (LO) phonons becomes important (Fig. 6). It should be noted that, although the coupling between the ground state and the LO modes is strongly reduced by charge cancellation, effects involving higher (dark) exciton states may still have considerable impact [30,53]. First, let us note that the interaction energy for LO phonons is comparable with their frequencies which results in a pronounced reconstruction of the spectrum and appearance of polaron states [11,14,20] which, due to strong non-diagonal couplings, mix various excitonic levels. This is manifested in the redistribution of the exciton occupation among different states even for arbitrarily long and weak pulses, where the dynamical contribution from the LO phonons vanishes (Fig. 6c). It may be easily verified that in the limit of slow rotation, when $K_{sc}(\omega) \rightarrow 0$ for $\omega > 1$, the "static" occupation of the higher states is equal to the usual perturbative correction to the state $j=1$. When $S_a(\omega)$ are sufficiently broad, i.e. for very short pulses or for large number of rotations, the terms $\omega > 1$ contribute also dynamically. The effect depends on the relative positions of the narrow LO phonon features and of the induced dynamics frequencies and the occupation of the excited states is a non-monotonous function of the pulse duration, due to the oscillatory character of the spectral functions $S_a(\omega)$ [35]. As seen in Fig. 6, for $\tau_p = 0.09$ ps, the frequency of induced dynamics overlaps with the phonon frequencies, leading

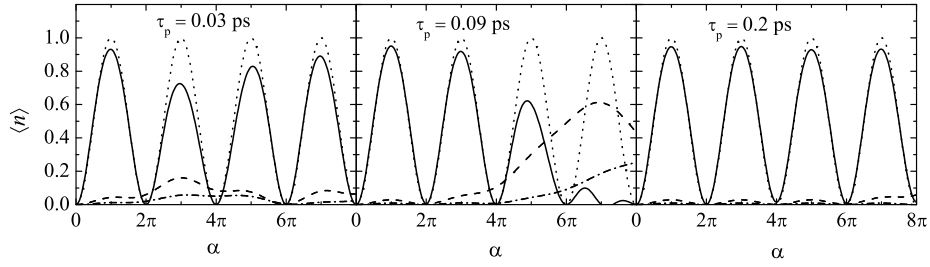


Figure 6: Pulse-intensity-dependent Rabi oscillations for sub-picosecond pulse durations as shown; solid: ground state, dashed: $M = 1; N = 0$, dash-dotted: $M = 2; N = 0$, dotted: ideal oscillation), where M denotes angular momentum, N .

to large damping. For longer durations it shifts towards lower frequencies, decreasing the impact on the system dynamics. However, the damping is weaker also for shorter durations ($\tau_p = 0.03$, Fig. 6a): e.g. for $\alpha = 6\pi$ the largest maximum is now to the right of the reservoir response frequencies $\omega_1 + \omega_L$, while for lower values of α the magnitude of the spectral functions $S_{a\phi,c}$ is smaller.

Conclusion. The above analysis shows that damping of pulse-area-dependent Rabi oscillations due to interaction with lattice modes is a fundamental effect of non-Markovian character: it is due to a semiclassical resonance between the optically induced confined charge dynamics and the lattice modes. The destructive effect may be minimized both by speeding up and slowing down the dynamics. However, in the former case, the system passes through unstable (decohering) states. Moreover, fast operation on a real system induces many undesirable effects: transitions to higher states, bi-exciton generation or resonant LO phonon dynamics. On the other hand, for slow operation, the number of "good" oscillations is limited. Thus, it is impossible to perform an arbitrary number of fully coherent Rabi oscillations on an exciton confined in a quantum dot.

By increasing the pulse duration as $\tau_p \propto \alpha^2$, the phonon effect on the exciton dynamics may be kept constant. However, in this case the achievable number of oscillations is strongly restricted by the exciton lifetime and other (thermally activated) processes. Eliminating the radiative losses e.g. by using stimulated Raman adiabatic passage instead of a simple optical excitation [40] seems to be a promising direction from this point of view.

The model presented above accounts for the decrease of the quality of Rabi oscillations in the short duration range observed in the experiment [5]. It predicts, however, that this trend is reversed for longer pulse durations. The quantitative value of 96% for the first maximum of the oscillations with $\tau_p = 1$ ps agrees very well with the experimental result [4] although the following extrema are much worse in reality than predicted here. This suggests an increased lattice response at higher frequencies which may be due to more complicated wavefunction geometry [22] or electric-field induced charge separation leading to strong piezoelectric effects [29]. Nevertheless, as far as it may be inferred from the experiment [4], the decrease of the oscillation quality seems to saturate after one full Rabi rotation, as predicted by the model calculations.

7 Optimal control over a QD qubit

Introduction. As we have already pointed out, any fast change of the state of the carrier subsystem leads to spontaneous processes of lattice relaxation that affect the coherence of the carrier state. In the previous section we have shown that coherent control is recovered if the evolution of the carrier subsystem is slow (adiabatic) compared to the typical timescales of the lattice dynamics. Thus, the requirement to avoid traces of the carrier dynamics in the outside world favors slow operation on the carrier subsystem, contrary to other decoherence processes (of Markovian character),

like radiative decay of the exciton or thermally activated processes of phonon-assisted transitions to higher states. The latter have the character of an exponential decay and, for short times, contribute an error $\sim \tau_g = \tau_d$, where τ_g is the gating time and τ_d is the time constant of the decay. Means to minimize this contribution by speeding up the control operation have been proposed by selecting materials to provide favorable spectrum characteristics [10] or by applying techniques reducing unwanted transitions [54,55].

In this section we consider the interplay between these two contributions to the error for the solid-state qubit implementation using excitonic (charge) states in quantum dots (QDs) [37], with computational states defined by the absence (|0>) or presence (|1>) of one exciton in the ground state of the dot, operated by resonant coupling to laser light. We show that it leads to a trade-off situation with a specific gating time corresponding to the minimum decoherence for a given operation [56].

The system and its model. Since it has been shown experimentally [28] that coherence of superpositions induced by short pulses is unstable, it seems reasonable to perform operations on dressed states, i.e. on the correctly defined quasiparticles of the interacting carrier-phonon system [57]. This may be formally achieved by employing the solid-state-theory concept of adiabatic switching on the interaction (as done in [36], cf. [58]) to transform the states of the noninteracting system into the states of the interacting one. Thus, we assume adiabatic switching on/off of the interaction with phonons by appending the appropriate exponent to the original interaction Hamiltonian,

$$H_{int} = e^{-\tau_j} \sum_k F_k b_k^\dagger + F_k b_k e^{-\tau_j}; \quad (62)$$

where $\tau_j = 0^+$. F_k are the deformation potential coupling constants between the ground excitonic state and the longitudinal acoustical phonons (20) (this is the only contributing interaction mechanism for the timescales discussed here). The operator S now becomes

$$S(t) = U_C(t) e^{-\tau_j} U_C^\dagger(t);$$

where the free evolution operator is obtained from (27) by truncation to the two lowest states. The general formula (47) may now be used with the bare state $|j_0\rangle$. The adiabatic procedure assures that it is transformed to the dressed state before comparing it to the density matrix, so that the density is defined with respect to the stable, dressed states.

The irreversible error. The form of the operator $Y(!) = Y_{11}(!)$ is obtained in the same way as in the previous section. The only difference with respect to (48) is that the oscillating terms now vanish in the long-time limit, due to the adiabatic switching on/off described above. For the present purpose it is convenient to write the result in the form

$$Y(!) = \frac{1}{!} F(!) (|1\rangle\langle 0| - |0\rangle\langle 1| + |0\rangle\langle 0| - |1\rangle\langle 1|) + \frac{1}{!} F(!) (|0\rangle\langle 1| - |1\rangle\langle 0| + |0\rangle\langle 0| - |1\rangle\langle 1|);$$

where

$$F(!) = \sum_{i=1}^Z \frac{1}{!} \frac{d}{d!} e^{i!} e^{i!};$$

Since in the quantum information processing applications the initial state of the quantum bit is in general not known, it is reasonable to consider the error averaged over all input states. Let us introduce the function

$$S(!) = \text{Tr} \{ Y(!) \rho_0 \}^2;$$

where $|j_0\rangle$ is a state orthogonal to $|j_0\rangle$ and the average is taken over the Bloch sphere. By restricting (47) to the two-level case, the average error may now be written

$$= \frac{1}{4\pi} \int d\Omega R(\Omega) S(\Omega); \quad (63)$$

where $R(\Omega) = R_1^{(D,P)}(\Omega)$.

The averaging is most conveniently performed by noting that

$$Y(\Omega) = \frac{1}{4\pi} F(\Omega) j_{\frac{1}{2}} + \frac{1}{4\pi} F(-\Omega) j_{\frac{1}{2}} + j_{\frac{1}{2}}$$

where $j_{\frac{1}{2}} = (j_0 - j_1)/2$. Choosing

$$j_0 = \cos \frac{\theta}{2} e^{i\phi} + e^{i\phi'} \sin \frac{\theta}{2} j_{\frac{1}{2}}; \quad j_1 = \sin \frac{\theta}{2} e^{i\phi} - e^{i\phi'} \cos \frac{\theta}{2} j_{\frac{1}{2}};$$

one gets

$$S(\Omega) = F(\Omega) e^{i\phi'} \cos^2 \frac{\theta}{2} + F(-\Omega) e^{i\phi'} \sin^2 \frac{\theta}{2};$$

which, upon averaging over the angles θ, ϕ' on the Bloch sphere, leads to

$$S(\Omega) = \frac{1}{12} [F(\Omega)^2 + F(-\Omega)^2];$$

Let us now consider a Gaussian pulse for performing the quantum gate,

$$f(t) = \frac{1}{\sqrt{2\pi} p} e^{-\frac{1}{2} (t-p)^2}$$

Here p is the gate duration, while θ is the angle determining the gate, e.g. $\theta = \pi/2$ is the Hadamard gate, while $\theta = \pi$ is X (bit flip). The function $F(\Omega)^2$ that carries all needed information about spectral properties of the system's dynamics may be approximately written as

$$F(\Omega)^2 \approx 2 e^{-\frac{\Omega^2}{2p}} e^{-\frac{\Omega^2}{2p}}; \quad (64)$$

As may be seen from (63) and (64), for a spectral density $R(\Omega) \propto \Omega^n$ the error scales with the gate duration as p^{n+1} and p^{n+2} at low and high temperatures, respectively. Therefore, for $n > 2$ (typical e.g. for various types of phonon reservoirs, see section 3) the error grows for faster gates. Assuming the spectral density of the form $R(\Omega) = R_{DP} \Omega^3$ for low frequencies [in accordance with (25) at $T = 0$], we obtain from (63) and (64)

$$= \frac{1}{12} R_{DP} p^2; \quad \text{at } T = 0$$

This leading order formula holds for $p \gg 1$. Also, if we introduce the upper cut-off, the error will be finite even for an infinitely fast gate (see Fig. 4); this is the ultrafast limit discussed in Section 4.

Trade-off between two types of decoherence. As we have shown, in our model the error grows as the speed of gate increases. This could result in obtaining arbitrarily low error by choosing suitably low speed of gates. However, if the system is also subject to other types of noise this becomes impossible. Indeed, assuming an additional contribution growing with rate Γ_M , the total error per gate is

$$= \frac{\Gamma_M}{2} + \Gamma_M p; \quad \Gamma_M = \frac{1}{12} R_{DP}; \quad \Gamma_M = \frac{1}{\tau}; \quad (65)$$

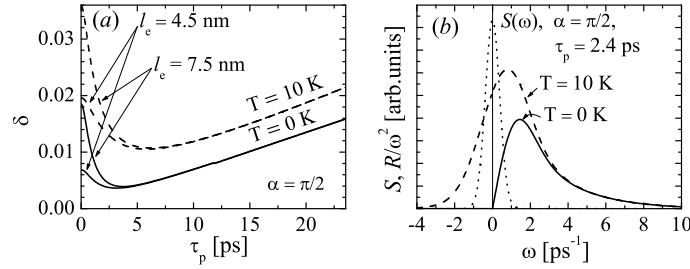


Figure 7: (a) Combined Markovian and non-Markovian error for a $\pi/2$ rotation on a qubit implemented as a confined exciton in a InAs/GaAs quantum dot, for $T = 0$ (solid lines) and $T = 10$ K (dashed lines), for two dot sizes (dot height is 20% of its diameter). The Markovian decoherence times are inferred from the experimental data [28]. (b) Spectral density of the phonon reservoir $R(\omega)$ at these two temperatures and the gate profile $S(\omega)$ for $\pi/2$.

where τ_r is the characteristic time of Markovian decoherence (recombination time in the excitonic case). As a result, the overall error is unavoidable and optimization is needed. The formulas (65) lead to the optimal values of the form (for $T = 0$)

$$\tau_{\min} = \frac{3}{2} \frac{2^2 R_{DP}}{3^2 \tau_r^{1=3}}; \text{ for } \tau_p = \frac{2}{3} 2^2 R_{DP} \tau_r^{1=3}; \quad (66)$$

For the specific material parameters of GaAs, the optimal gate time and minimal decoherence resulting from Eqs. (66) are

$$\tau_p = 2^3 1.47 \text{ ps}; \quad \tau_{\min} = 2^3 0.0035;$$

The exact solution within the proposed model, taking into account the cut-off and anisotropy (at shape) of the dot and allowing finite temperatures, is shown in Fig. 7. The size-dependent cut-off is reflected by a shift of the optimal parameters for the two dot sizes: larger dots admit faster gates and lead to lower error.

It should be noted that these optimal times are longer than the limits imposed by level separation [37,54,55]. Thus, the non-Markovian reservoir effects (dressing) seem to be the essential limitation to the gate speed.

Error reduction by a double-dot encoding. As we have seen, for long enough pulses the fidelity of a one-qubit rotation depends on the low-frequency behavior of the phonon spectral density. In this section we will show that for a different encoding of the quantum logical states this behavior can be made more favorable, even without changing to a different material. To be specific, we consider a qubit encoded by a single exciton in a double-dot system, with the logical values corresponding to the exciton location in one or the other dot. The physical reason for the weaker lattice impact at low frequencies is that phonons with wavelengths longer than the distance between the dots cannot distinguish between the two exciton positions and, therefore, cannot contribute to decoherence.

As in the preceding subsections, we restrict the discussion to the two states, denoted $|j\rangle_i$ and $|\bar{j}\rangle_i$, corresponding to the exciton position in one of the two QDs. We assume that it is possible to perform rotations in this space, analogous to the resonantly optically driven rotations of the single-dot excitonic qubit discussed above. Then, the qubit Hamiltonian H_C is again the 2-dimensional restriction of (5) with $\tau_1 = 0$. The interaction Hamiltonian is

$$H_{\text{int}} = |j\rangle_i \langle j| \sum_k F_k^{(0)} b_k^\dagger + F_k^{(0)} b_k + |\bar{j}\rangle_i \langle \bar{j}| \sum_k F_k^{(1)} b_k^\dagger + F_k^{(1)} b_k; \quad (67)$$

where $F_k^{(0;1)}$ are the coupling constants for the two exciton localizations. Again, we include only the DP coupling and suppress the corresponding upper index (DP). Let us assume that the dots are placed at $z = D/2$. If we neglect the possible differences between the geometry of wavefunctions in these dots then, according to the definitions (9) and (10), the coupling constants differ only by a phase factor,

$$F_k^{(0;1)} = e^{ik_z D/2} F_k;$$

where F_k are the coupling constants for an exciton located at the origin.

With the help of the Weyl operator

$$W = \exp \left(\sum_k b_k b_k^\dagger \right); \quad b_k = \frac{F_k^{(0)}}{\sqrt{F_k^{(0)}}}; \quad (68)$$

we define the new bosonic operators

$$b_k = W b_k W^\dagger = b_k; \quad (69)$$

In terms of these, the interaction Hamiltonian has the form (up to a constant)

$$H_{\text{int}} = e \sum_k b_k b_k^\dagger F_k^{(0)} + F_k^{(1)} b_k; \quad (70)$$

where

$$F_k^{(1)} = F_k^{(0)} \sin \frac{k_z D}{2}; \quad (71)$$

The physical meaning of the above manipulation is that the lattice excitations are now defined with respect to the new equilibrium, corresponding to the presence of the exciton in one of the dots. Again, we have introduced the factor describing the adiabatic switching on/off of the carrier-phonon interaction.

The interaction Hamiltonian is now formally identical to that used in the previous subsection, but the spectral density now is

$$R(\omega) = R_{\text{DP}} \frac{1}{3} \left(\frac{D}{c_l} \right)^2 \omega^5 [n_B(\omega) + 1] g(\omega);$$

where $g(0) = 1$. The non-Markovian error for sufficiently long gate durations at $T = 0$ may now be estimated as

$$= \frac{1}{12} R_{\text{DP}} \left(\frac{1}{3} \left(\frac{D}{c_l} \right)^2 \right)^4;$$

Compared to the corresponding value for the simple encoding (65), this shows much faster decrease with growing pulse duration. By combining this error with the Markovian decoherence rate resulting from the natural exciton lifetime and optimizing with respect to the pulse duration one finds

$$\epsilon_{\text{min}} = \frac{5}{4} \left(\frac{2}{9} R_{\text{DP}} \left(\frac{D}{c_l} \right)^2 \right)^{1/5}; \quad \text{for } \tau_p = \left(\frac{2}{9} R_{\text{DP}} \left(\frac{D}{c_l} \right)^2 \right)^{1/5};$$

The comparison of the error with single- and double-dot encoding at $T = 10$ K is shown in Fig. 8, with the exciton decay time the same as in the previous subsection. For the double-dot encoding, the error is lower by a factor of 3 and the optimal gating time is shifted to lower values.

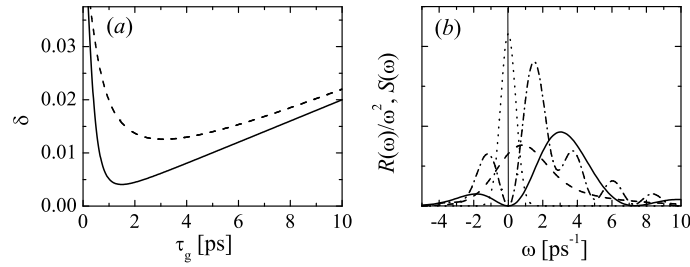


Figure 8: (a) Combined Markovian and non-Markovian error for a $\pi/2$ rotation on a qubit implemented as a confined exciton in a double InAs/GaAs quantum dot separated by $D = 5$ nm for $T = 10$ K (solid line), and for the simple encoding (dashed line). (b) The spectral densities of the phonon reservoir at $T = 10$ K (solid: $D = 5$ nm, dot-dashed: $D = 15$ nm, dashed: single dot) and the nonlinear pulse spectrum (dotted). The wavefunction width was taken to be 4.5 nm in-plane and 0.9 nm in the growth direction. The difference between electron and hole localization widths has been neglected.

8 Fidelity of a STIRAP qubit

Introduction. As we have shown in the preceding sections, the fidelity of quantum information processing schemes implemented on orbital (excitonic) degrees of freedom is limited due to the finite exciton lifetime, usually of order of 1 ps [28,50], and to the adiabaticity requirement excluding unlimited speed-up of the operation. On the other hand, spin-based proposals [59], favored by the long lifetime of electron spin [60] also suffer from serious difficulties: the spin switching time in typical structures is very long due to weak magnetic coupling. It seems therefore natural to seek for a scheme in which the logical values are stored using spin states, while the operations are performed via optical coupling to the charge degrees of freedom [38,42,39,41].

Recently, it was proposed [40] to encode the qubit into spin states of a single excess electron in a QD and perform an arbitrary rotation [61] by employing the stimulated Raman adiabatic passage (STIRAP) to a state localized spatially in a neighboring dot [62]. Although this passage requires coupling to a charged exciton (X^- , or trion) state which has a finite lifetime, this state is never occupied (in the ideal case) so that the scheme is not affected by the decoherence resulting from its decay.

From the discussion presented in the previous sections of this chapter it is clear that the solid state QD structures, where the new implementation of these quantum-optical schemes is proposed, differ essentially from the atomic systems, where these procedures are successfully applied [63]. It may be expected that the coupling to the lattice modes will play an important role in such sophisticated quantum control schemes, restricting the range of parameters, where the coherent transfer may be performed with high fidelity.

In these section we briefly discuss the phonon effects on a STIRAP qubit. The complete discussion exceeds the scope of this chapter and may be found in [64].

The Raman adiabatic passage. The arbitrary rotation of the spin qubit between the states $|j_1\rangle$ and $|j_2\rangle$ (different spin orientations in one dot) may be performed with the help of an auxiliary state $|j_3\rangle$ [61] (electron in another dot). All these three states are coupled to a fourth state (trion) $|j_4\rangle$ by laser beams $\omega_0; \omega_1; \omega_2$. In order to achieve the Raman coupling, the detunings from the corresponding dipole transition energies must be the same for all the three laser frequencies. Therefore, we put $\Delta_n = \omega_3 - \omega_n$, $n = 0; 1; 2$. The envelopes of the first two pulses are proportional to each other,

$$\omega_0(t) = \omega_1(t) \cos \theta; \quad \omega_1(t) = \omega_1(t) \sin \theta; \quad \omega_2(t) = \omega_2(0; \frac{\pi}{2}):$$

Upon transition to the "rotating" basis $\tilde{p}_i = e^{i(\omega_n t - \tilde{\phi}_n)} p_i$, $\tilde{\phi}_n = \phi_n - \omega_n t$, $n = 0, 1, 2$ and suppressing the constant term, the RWA Hamiltonian may be written

$$H_C = \tilde{p}_{i3} \tilde{p}_{j+} + \frac{1}{2} \omega_1(t) (\tilde{p}_{i3} \tilde{p}_{j+} + \tilde{p}_{i1} \tilde{p}_{j-}) + \frac{1}{2} \omega_2(t) (e^{i\tilde{\phi}_2} \tilde{p}_{i3} \tilde{p}_{j+} + e^{-i\tilde{\phi}_2} \tilde{p}_{i1} \tilde{p}_{j-}) : \quad (72)$$

where

$$\tilde{p}_i = \cos \tilde{\phi}_i + e^{i\tilde{\phi}_1} \sin \tilde{\phi}_i; \quad \tilde{p}_{i+} = \sin \tilde{\phi}_i + e^{i\tilde{\phi}_1} \cos \tilde{\phi}_i;$$

Hence, the pulses affect only one linear combination of the qubit states, the coupled (bright) state \tilde{p}_i , while the other orthogonal combination, \tilde{p}_{i+} , remains unaffected. The Hamiltonian (72) has the eigenstates

$$\tilde{p}_{0i} = \cos \tilde{\phi}_i - e^{i\tilde{\phi}_2} \sin \tilde{\phi}_i; \quad (73)$$

$$\tilde{p}_{-i} = \cos (\sin \tilde{\phi}_i + e^{i\tilde{\phi}_2} \cos \tilde{\phi}_i) - \sin \tilde{\phi}_i; \quad (74)$$

$$\tilde{p}_{+i} = \sin (\sin \tilde{\phi}_i + e^{i\tilde{\phi}_2} \cos \tilde{\phi}_i) + \cos \tilde{\phi}_i; \quad (75)$$

where

$$\tan \tilde{\phi}_i = \frac{\omega_1}{\omega_2}; \quad \sin \tilde{\phi}_i = \frac{1}{\sqrt{2}} \frac{\omega_1}{\sqrt{\omega_1^2 + \omega_2^2}}; \quad \cos \tilde{\phi}_i = \frac{\omega_2}{\sqrt{\omega_1^2 + \omega_2^2}};$$

The corresponding eigenvalues are

$$\epsilon_0 = 0; \quad \epsilon_{\pm} = \frac{1}{2} \sqrt{\omega_1^2 + \omega_2^2}; \quad (76)$$

The system evolution is realized by adiabatic change of the pulse amplitudes (in this application, the detuning remains constant). Initially (at the times), both pulses are switched off, hence $\omega_1 = 0$, then ω_2 is switched on first, hence also $\omega_1 = 0$. Therefore, \tilde{p}_{0i} coincides with \tilde{p}_i and \tilde{p}_{-i} with \tilde{p}_{i+} . During adiabatic evolution of the parameters, the states move along the corresponding spectral branches. As shown in Ref. [61], performing the transfer from $\omega_1 = 0$ to $\omega_1 = \omega_2$ and then back with a different phase $\tilde{\phi}_2$ of the ω_2 pulse results in a rotation in the qubit space $\tilde{p}_i, \tilde{p}_{i+}$ around the axis determined by $\tilde{\phi}_1$ and by the relative phase $\tilde{\phi}_2$ between ω_1 and ω_2 . The rotation angle is equal to the difference of the $\tilde{\phi}_2$ phases in the first and second pulse sequence. Ideally, the state \tilde{p}_i is only occupied during gating, while the state \tilde{p}_{i+} is never occupied.

The above procedure works under assumption that the evolution is perfectly adiabatic. However, any change of parameters can never be infinitely slow and the probability of a jump from \tilde{p}_{0i} to one of the two other states $\tilde{p}_{\pm i}$ remains finite, leading to non-vanishing occupation of the trion state and to decoherence. In order to avoid this error, one has to impose the usual adiabaticity condition

$$\dot{\tilde{\phi}}_i \ll \omega_{\pm}; \quad (77)$$

where ω_{\pm} is the duration of the process.

Phonon-induced decoherence. In the presence of phonons, the fundamental adiabaticity condition (77) is supplemented by the additional requirement to avoid phonon-assisted processes. It may be shown [64] that the only phonon coupling term that contributes at the leading order of the perturbation is

$$H_{int} = \sum_k \tilde{p}_{i2} \tilde{p}_{j-} (F_k b_k + b_k^\dagger); \quad (78)$$

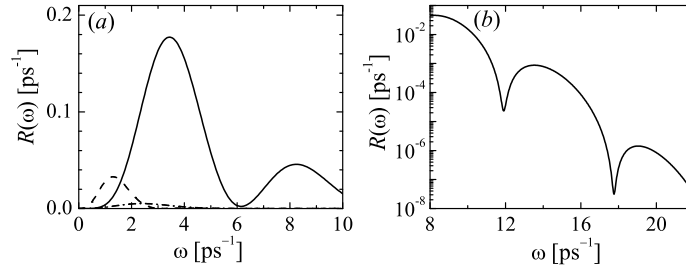


Figure 9: (a) The contributions to the spectral density at $T = 0$: DP coupling to LA phonons (solid) and piezoelectric coupling to TA (dashed) and LA (dash-dotted) phonons. (b) The high-frequency behavior of the DP contribution.

where F_k is obtained in the way analogous to (71) by shifting the phonon modes to the equilibrium appropriate to the occupation of the first dot (states $|j_i; j_l\rangle$). This time, however, coupling constants for a single electron must be used. Vanishing of all the other contributions results from the indistinguishability of spin states by phonon interactions, from the large mismatch between the trion creation energy and phonon energies and from the fact that the state $|j_l\rangle$ is not occupied in the ideal case. Since now the single, uncompensated charge carrier is shifted between different spatial locations, one may expect a considerable contribution from the piezoelectric coupling to acoustical phonons. Indeed, as shown in Fig. 9, this coupling dominates at low frequencies, while for high frequencies it decreases rather fast due to vanishing geometrical factors (14{16) in the strongest conformation direction. In the high-frequency sector, the deformation potential coupling dominates, with the oscillatory tail characteristic to a double-dot structure.

Even though H_{int} (78) is diagonal in the bare carrier states, it still gives rise not only to the pure dephasing effect discussed in the section 7 but also to transitions between the trapped carrier-eld states (73{75). The probability of these phonon-induced transitions becomes very high if the spacing between the trapped energy levels falls into the area of high phonon spectral density and the contribution to the error resulting from such transitions is approximately proportional to the process duration,

$$R(\omega) \approx \frac{1}{\omega} \quad (79)$$

with some additional effects appearing due to the pure-dephasing broadening of the levels if they are placed in the narrow local minima in the tail of $R(\omega)$. These strong decoherence processes may be avoided by either decreasing the trapped level separation (low-frequency regime, exploiting the $1/\omega$ behavior of spectral densities for $\omega \rightarrow 0$) or increasing it beyond the cut-off (high frequency regime). In both cases one encounters a trade-off situation, due to the opposite requirements for phonon-induced jumps (short duration) and for the fundamental adiabaticity condition and pure dephasing (slow operation): In the low-frequency regime, avoiding phonon-induced transitions contradicts the condition for avoiding non-adiabatic jumps between the trapped states, which may be overcome only by considerably extending the process duration. In the high-frequency case, there is competition between the pure dephasing and the phonon-induced transitions that is overcome by increasing the trapped state splitting, taking advantage of the particular structure of the phonon spectral density for a double dot structure.

In order to provide some quantitative estimations of the error, in Fig. 10 we present the result of the numerical optimization of the pulse parameters for $j_l - j_i$ located at the minima of $R(\omega)$ around 6 ps^{-1} and 12 ps^{-1} [64]. It turns out that a very high fidelity may be achieved for reasonable pulse parameters and for acceptable duration of the control sequence (note that τ_0 is a measure of duration of a single transfer; taking into account two transfers which should be well separated in time leads to the total duration which is roughly ten times longer).

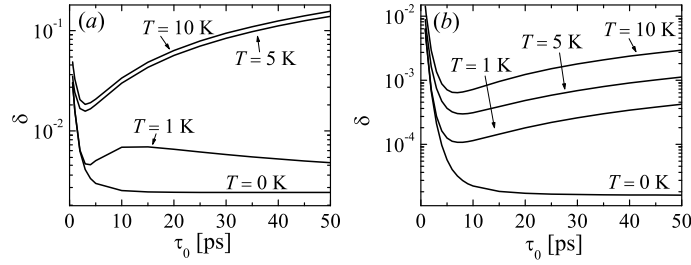


Figure 10: The minimum achievable error as a function of the transfer duration corresponding to the optimal pulse parameters with both γ and β in the minimum of $R(\beta)$ at 6 ps^{-1} (a) and at 12 ps^{-1} (b).

9 Conclusions

We have discussed phonon-related corrections to externally controlled quantum coherent dynamics of carriers confined in quantum dots. We have shown that the carrier-phonon interaction leads to lattice relaxation (dressing process) after a change of the carrier state. This relaxation process leads to entanglement between the carrier and lattice subsystems and thus to decoherence of the carrier states.

In order to discuss the possible reduction of this decoherence effect by slowing down the carrier dynamics, we have developed a perturbative method for calculating the phonon corrections to arbitrary evolution. This method allows one to qualitatively predict the phonon effect based on the nonlinear spectral properties of the induced carrier dynamics and on the general knowledge of the spectral properties of the lattice modes.

With this approach, we have studied the Rabi oscillations of exciton occupation in a QD. We have shown that the lattice response is resonantly driven by a combination of the (linear) pulse spectrum and the Rabi frequency. It turns out that the quality of the oscillations improves both for fast and for slow dynamics, but only in the latter case the intermediate states are stable.

Applying the perturbative procedure to a QD implementation of a quantum bit we have shown that the error for a single-qubit operation may be decreased when one approaches the adiabatic limit, in which the lattice modes reversibly follow the carrier evolution. This requires, however, long process durations, which increases the contribution from other decoherence mechanisms. As a result of the interplay between these two contributions, a specific pulse duration appears which optimizes the fidelity of the process. The error may be slightly reduced if the simple qubit encoding in a single QD is replaced by a double-dot encoding, with qubit values defined by the exciton position in one of the dots.

Finally, we have discussed the phonon impact on the rotation of a spin qubit performed optically by adiabatic Raman transition. It turns out that by a suitable choice of parameters, such a procedure may be performed with very a high fidelity in a reasonable time.

The presented results show that phonon-related decoherence processes form the essential limitation to the coherent manipulation of confined carrier states in quantum dots. However, by employing more and more sophisticated control techniques the resulting error may be substantially reduced. With the help of theoretical modeling presented in this chapter it is possible to optimize both the system properties and the operational parameters in order to maximize the fidelity of quantum coherent control.

Acknowledgments. Supported by the Polish Ministry of Scientific Research and Information Technology under the (solicited) Grant No. PBZ-MIN-008/P03/2003 and by the Polish KBN under Grant No. PB 2 P 03B 085 25. P.M. is grateful to the Humboldt Foundation for Support.

References

- [1] N. N. Bonadeo, J. Erland, D. Gammon, D. S. Katzer, D. Park, and D. G. Steel, *Science* 282, 1473 (1998).
- [2] T. H. Stievater, X. Li, D. G. Steel, D. Gammon, D. S. Katzer, D. Park, C. Piermarocchi, and L. J. Sham, *Phys. Rev. Lett.* 87, 133603 (2001).
- [3] H. Kamada, H. Gotoh, J. Temmyo, T. Takagahara, and H. Ando, *Phys. Rev. Lett.* 87, 246401 (2001).
- [4] A. Zrenner, E. Beham, S. Stuerner, F. Findeis, M. Bichler, and G. Abstreiter, *Nature* 418, 612 (2002).
- [5] P. Borri, W. Langbein, S. Schneider, U. Woggon, R. L. Sellin, D. Ouyang, and D. Bimberg, *Phys. Rev. B* 66, 081306 (2002).
- [6] H. Htoon, T. Takagahara, D. Kulik, O. Baklenov, A. L. Holmes Jr., and C. K. Shih, *Phys. Rev. Lett.* 88, 087401 (2002).
- [7] M. Bayer, P. Hawrylak, K. Hinzer, S. Fafard, M. Korkusinski, Z. R. Wasilewski, O. Stem, and A. Forchel, *Science* 291, 451 (2001).
- [8] G. D. Mahan, *Many-Particle Physics*, Kluwer, New York (2000).
- [9] U. Hohenester, R. DiFelice, E. Molinari, and F. Rossi, *Physica E* 7, 934 (2000).
- [10] S. De Rinaldis, I. D'Amico, E. Biolatti, R. Rinaldi, R. Cingolani, and F. Rossi, *Phys. Rev. B* 65, 081309 (2002).
- [11] S. Hamau, Y. Guldner, O. Verzelen, R. Ferreira, G. Bastard, J. Zeman, A. Lematre, and J. M. Gerard, *Phys. Rev. Lett.* 83, 4152 (1999).
- [12] S. Hamau, J. N. Isaia, Y. Guldner, E. Deleporte, O. Verzelen, R. Ferreira, G. Bastard, J. Zeman, and J. M. Gerard, *Phys. Rev. B* 65, 085316 (2002).
- [13] O. Verzelen, R. Ferreira, and G. Bastard, *Phys. Rev. Lett.* 88, 146803 (2002).
- [14] L. Jacak, J. Kasnyj, D. Jacak, and P. Machnikowski, *Phys. Rev. B* 67, 035303 (2003).
- [15] R. Heitz, M. Veit, N. N. Ledentsov, A. Homann, D. Bimberg, V. M. Ustinov, P. S. Kop'ev, and Z. I. Alferov, *Phys. Rev. B* 56, 10435 (1997).
- [16] R. Heitz, H. Bom, F. Gueth, O. Stier, A. Schliwa, A. Homann, and D. Bimberg, *Phys. Rev. B* 64, 241305 (2001).
- [17] I. V. Ignatiev, I. E. Kozin, V. G. Davydov, S. V. Nair, J.-S. Lee, H.-W. Ren, S. Sugou, and Y. Masumoto, *Phys. Rev. B* 63, 075316 (2001).
- [18] X.-Q. Li, H. Nakayama, and Y. Aikawa, *Phys. Rev. B* 59, 5069 (1999).
- [19] O. Verzelen, R. Ferreira, and G. Bastard, *Phys. Rev. B* 62, R4809 (2000).
- [20] L. Jacak, J. Kasnyj, D. Jacak, and P. Machnikowski, *Phys. Rev. B* 65, 113305 (2002).
- [21] O. Verzelen, G. Bastard, and R. Ferreira, *Phys. Rev. B* 66, 081308 (2002).
- [22] R. Heitz, I. Mukhametzhanov, O. Stier, A. M. Adhukar, and D. Bimberg, *Phys. Rev. Lett.* 83, 4654 (1999).
- [23] R. Heitz, I. Mukhametzhanov, O. Stier, A. M. Adhukar, and D. Bimberg, *Physica E* 7, 398 (2000).
- [24] A. Lematre, A. D. Ashmore, J. J. Finley, D. J. Mowbray, M. S. Skolnick, M. Hopkinson, and T. F. Krauss, *Phys. Rev. B* 63, 161309 (2001).
- [25] F. Findeis, A. Zrenner, G. Bohm, and G. Abstreiter, *Phys. Rev. B* 61, R10579 (2000).
- [26] V. M. Fomin, V. N. Gladilin, S. N. Klimin, J. T. Devreese, P. M. Koenraad, and J. H. Wolter, *Phys. Rev. B* 61, R2436 (2000).
- [27] L. Jacak, J. Kasnyj, and W. Jacak, *Phys. Lett. A* 304, 168 (2002).
- [28] P. Borri, W. Langbein, S. Schneider, U. Woggon, R. L. Sellin, D. Ouyang, and D. Bimberg, *Phys. Rev. Lett.* 87, 157401 (2001).
- [29] B. Krummheuer, V. M. Axt, and T. Kuhn, *Phys. Rev. B* 65, 195313 (2002).
- [30] L. Jacak, P. Machnikowski, J. Kasnyj, and P. Zoller, *Eur. Phys. J. D* 22, 319 (2003).
- [31] A. Vagov, V. M. Axt, and T. Kuhn, *Phys. Rev. B* 66, 165312 (2002).
- [32] A. Vagov, V. M. Axt, and T. Kuhn, *Phys. Rev. B* 67, 115338 (2003).
- [33] J. Forstner, C. Weber, J. Dankwerts, and A. Knorr, *Phys. Rev. Lett.* 91, 127401 (2003).
- [34] P. Machnikowski and L. Jacak, *Phys. Rev. B* 69, No. 19 (2004), in press, cond-mat/0305165.
- [35] P. Machnikowski and L. Jacak, *Semicond. Sci. Technol.* 19, S299 (2004), cond-mat/0307615.
- [36] R. Alicki, M. Horodecki, P. Horodecki, and R. Horodecki, *Phys. Rev. A* 65, 062101 (2002). quant-ph/0105115.
- [37] E. Biolatti, R. C. Iotti, P. Zanardi, and F. Rossi, *Phys. Rev. Lett.* 85, 5647 (2000).

- [38] A. Imamoglu, D. D. Awschalom, G. Burkard, D. P. Divincenzo, D. Loss, M. Sherwin, and A. Small, *Phys. Rev. Lett.* **83**, 4204 (1999).
- [39] E. Pazy, E. Biolatti, T. Calarco, I. D'Amico, P. Zanardi, F. Rossi, and P. Zoller, *Europhys. Lett.* **62**, 175 (2003).
- [40] F. Troiani, E. Molinari, and U. Hohenester, *Phys. Rev. Lett.* **90**, 206802 (2003).
- [41] T. Calarco, A. Datta, P. Fedichev, E. Pazy, and P. Zoller, *Phys. Rev. A* **68**, 12310 (2003).
- [42] M. Feng, I. D'Amico, P. Zanardi, and F. Rossi, *Phys. Rev. B* **67**, 014306 (2003).
- [43] Pochung Chen, C. Piermarocchi, L. J. Sham, D. Gammon, and D. G. Steel, *Phys. Rev. B* **69**, 075320 (2004).
- [44] X. Li, Y. W. D. Steel, D. Gammon, T. Stievater, D. Katzer, D. Park, C. Piermarocchi, and L. Sham, *Science* **301**, 809 (2003).
- [45] M. I. Vasilevskiy, R. P. Miranda, E. V. Anda, and S. S. M. Aklers, *Semicond. Sci. Technol.* **19**, S312 (2004).
- [46] H. Haken, *Quantum Field Theory of Solids. An Introduction*, North-Holland, Amsterdam (1976).
- [47] G. D. Mahan, *Polarons in heavily doped semiconductors*, in: J. T. Devreese, editor, *Polarons in Ionic Crystals and Polar Semiconductors*, North-Holland, Amsterdam (1972).
- [48] F. Vallee and F. Bogani, *Phys. Rev. B* **43**, 12049 (1991).
- [49] F. Vallee, *Phys. Rev. B* **49**, 2460 (1994).
- [50] M. Bayer and A. Forchel, *Phys. Rev. B* **65**, 041308 (2002).
- [51] C. Cohen-Tannoudji, J. Dupont-Roc, and G. Grynberg, *Atom-Phonon Interactions*, Wiley-Interscience, New York (1998).
- [52] V. M. Axt, M. Herbst, and T. Kuhn, *Superlattices and Microstructures* **26**, 118 (1999).
- [53] V. M. Fomin, V. N. Gladilin, J. T. Devreese, E. P. Pokatilov, S. N. Balaban, and S. N. Klimin, *Phys. Rev. B* **57**, 2415 (1998).
- [54] Pochung Chen, C. Piermarocchi, and L. J. Sham, *Phys. Rev. Lett.* **87**, 067401 (2001).
- [55] C. Piermarocchi, Pochung Chen, Y. S. Dale, and L. J. Sham, *Phys. Rev. B* **65**, 075307 (2002).
- [56] R. Alicki, M. Horodecki, P. Horodecki, R. Horodecki, L. Jacak, and P. Machnikowski, *Optimal strategy of quantum computing and trade-off between opposite types of decoherence*, quant-ph/0302058 (2003), submitted.
- [57] R. Alicki, *Decoherence in quantum open systems revisited*, quant-ph/0205173 (2002).
- [58] D. Pines and P. Nozieres, *The Theory of Quantum Liquids*, Addison-Wesley, Redwood (1989).
- [59] D. Loss and D. P. Divincenzo, *Phys. Rev. A* **57**, 120 (1998).
- [60] R. Hanson, B. Witkamp, L. M. K. Vandersypen, L. H. W. Hillemans van Beveren, J. M. Elzerman, and L. P. Kouwenhoven, *Phys. Rev. Lett.* **91**, 196802 (2003).
- [61] Z. Kis and F. Renzoni, *Phys. Rev. A* **65**, 032318 (2002).
- [62] U. Hohenester, F. Troiani, E. Molinari, G. Panzarini, and C. Macchiavello, *Appl. Phys. Lett.* **77**, 1864 (2000).
- [63] K. Bergmann, H. Teuer, and B. W. Shore, *Rev. Mod. Phys.* **70**, 1003 (1998).
- [64] K. Roszak, A. G. Rodecka, P. Machnikowski, and T. Kuhn, *Phonon-induced decoherence for a QD STIRAP qubit*, to be published (2004).